Cell Biol Toxicol (2019) 35:541–564
https://doi.org/10.1007/s10565-019-09467-7

ORIGINAL ARTICLE

Relevance of Erk1/2-PI3K/Akt signaling pathway in CEES-induced oxidative stress regulates inflammation and apoptosis in keratinocytes

Silpa Sabnam · **Arttatrana Pal**

Received: 27 November 2018 / Accepted: 13 February 2019 / Published online: 25 February 2019
© Springer Nature B.V. 2019

Abstract 2-Chloroethyl ethyl sulfide (CEES) is a well-known chemical warfare agent that induces cellular stress in exposed individuals. However, molecular mechanisms of CEES-induced oxidative stress–mediated metabolic deregulation are not clearly elucidated. Here we investigated CEES-induced free radical production act as key functional mediators of metabolic stress via Erk1/2 mitogen–activated protein kinases (MAPKs) and phosphatidylinositol-3-kinase (PI3K/Akt) signaling cascades in keratinocytes. We observed that CEES exposure disrupts the cellular antioxidant defense capacities leading to increase in free oxygen and nitrogen radical accumulation in keratinocytes. These unusual cellular abnormalities initiate cellular stress via Erk1/2-PI3K/Akt signaling pathways. Biochemical tools were used to analyze the changes in metabolites including sulfur amino acids (SAAs), namely, L-glutathione (GSH) and L-cysteine (Cys), in the presence of selective inhibitors of reactive oxygen/nitrogen species (ROS/RNS), Erk1/2, or PI3K/Akt after CEES exposure. Importantly, these metabolite changes were accompanied by a decrease in the glycolytic flux, consistent with the observed decrease in 6-phosphofructo-2-kinase/fructose-2,6-bisphosphatase (PFK-2) concentration and these CEES-induced phenomena were attenuated by pretreatment of Erk1/2 or PI3-K/Akt inhibitors. On the other hand, CEES exposure disrupts the protein carbonylation (PC) and lipid peroxidation (LPO) in keratinocytes leading to inflammation, crash of the cell–cell communication, cell cycle deregulation, and apoptosis via Erk1/2-PI3K/Akt pathways. However, pretreatment of Erk1/2 or PI3K/Akt inhibitors attenuated the CEES action. Collectively, these results illustrated that accumulated free radicals act as key functional mediators for inflammation, and apoptosis via Erk1/2-PI3K/Akt regulatory signaling cascades induced by CEES exposure. Treatment of pharmacological Erk1/2-PI3K/Akt inhibitors attenuated the CEES-induced keratinocyte injury that may provide the basis for the development of therapeutic strategy to work against CEES exposure.

Keywords CEES · Erk1/2-PI3K/Akt · Oxidative stress · Metabolites · Inflammation · Apoptosis

Introduction

Sulfur mustard (HD) is a vesicating agent and used as a potential chemical warfare by terrorist organization in a number of conflicts, posing a major threat in both military conflicts and chemical terrorism situations. Since

---

Electronic supplementary material The online version of this article (https://doi.org/10.1007/s10565-019-09467-7) contains supplementary material, which is available to authorized users.

S. Sabnam · A. Pal
School of Biotechnology, Kalinga Institute of Industrial Technology, Bhubaneswar 751024, India

A. Pal (✉)
Neurobiology Lab, Department of Zoology, School of Life Sciences, Mahatma Gandhi Central University, Motihari, Bihar 845401, India
e-mail: arttatrana@yahoo.com

HD is extremely *toxic contaminant*, research studies are generally being carried out with less toxic, monofunctional HD analog, CEES. Importantly, airway CEES exposure targets primarily skin, the cornea of the eye, and the respiratory organs. Studies have shown that CEES exposure to keratinocytes increases the oxidative stress leading to cellular complications in both animal and cell culture models (Gould et al. 2009; Tewari-Singh et al. 2009; Pal et al. 2009). Induction of oxidative stress by CEES exposure triggered activation of many transcription factors via upstream signaling pathways including MAPKs and PI3K/Akt in keratinocytes (Pal et al. 2009; Tewari-Singh et al. 2009, 2010, 2012). Mediating signal transduction from cell surface to the nucleus, the Erk1/2 and Akt are involved in the regulation of cellular fat–like inflammation, cell growth, or apoptosis (Shaulian and Karin 2001; Pal et al. 2009; Tewari-Singh et al. 2012). Recently, our studies have demonstrated that CEES-induced intracellular free radical accumulations triggered inflammation and apoptosis in macrophages via activation of redox-signaling pathways (Sagar et al. 2017). However, the definitive picture of the signals that trigger apoptosis leading to keratinocyte damage and the molecular pathways responsible for the development of keratinocyte complications is far from being elucidated.

Generation of NO in cellular compartments acts in a redox-dependent manner to counteract oxidative stress either by directly acting as an antioxidant through scavenging superoxide ($O_2{\cdot}-$), to form peroxynitrite (ONOO–), or by acting as a signaling molecule, and altering gene expression that triggers various physiological processes (Sagar et al. 2014). Peroxynitrite, a highly reactive nitrogen species, reacts with biomolecules of sub-cellular organelles in cellular compartments through oxidative/nitrosative mechanism. However, when endogenous NO productions are accelerated and antioxidant defenses become depleted, the cellular NO gives rise to secondary oxidizing species ONOO–, which can modulate the protein and lipid oxidation reactions (Sagar et al. 2017). On the other hand, low-molecular-mass antioxidant enzymes regenerating the reduced forms of antioxidants and ROS-interacting enzymes include glutathione peroxidase (GPx), GSH, and catalase (CAT) and loss of these antioxidants due to CEES exposure triggers oxidative/nitrosative stress (Sagar et al. 2017; Tewari-Singh et al. 2010).

Previously, many studies have reported that CEES exposure resulted in biomolecule damage such as DNA, lipids, and proteins, leading to inflammation and apoptosis both in vivo and in vitro models (Sagar et al. 2014, 2017; Pal et al. 2009). However, changes in the central carbon metabolic network were induced by Erk1/2 and PI3K/Akt inhibition and provide a tool to analyze the metabolic flux distribution in keratinocytes as cross talk between signal transduction and metabolic events. By tracking the changes in metabolic fluxes induced by Erk1/2 and PI3K/Akt signaling modulators, we hypothesized that CEES-induced partial cross talks between inflammatory signal transduction with metabolic networks are associated with small molecules present in keratinocytes. Arginine (Arg) is a conditionally essential amino acid whose nutritional requirement is increased during inflammation (Albina et al. 1990; Morris et al. 1998). During inflammation, Arg is catabolized primarily to citrulline (Cit) and ornithine (Orn) to generate NO, urea, and the polyamines putrescine (Put), spermidine (Spd), and spermine (Spm) in different pathophysiological conditions. The products of Arg catabolism directly modulate inflammation by controlling endothelial function, leukocyte recruitment and activation, innate immunity, and extracellular matrix remodeling (Morris et al. 1998). Moreover, metabolism of SAA occurs through four interconnected metabolic pathways such as transmethylation, transsulfuration, GSH synthesis, and the γ-glutamyl cycle (Brosnan and Brosnan 2006; Finkelstein 2006). Each of these cycles produces one sulfhydryl (–SH)-containing compound. These are homocysteine (Hcy), Cys, GSH, and cysteinylglycine (Cysgly). Moreover, Cys and γ-glutamylcysteine synthetase (GCS) are precursors to GSH (Pastore et al. 1998) and cysteinylglycine is derived from the breakdown of GSH *(*Meister 1983*)*. The homeostatic balance of these compounds is important for cellular redox regulation (Jones 2006; Schafer and Buettner 2001).

Recently, Tawakol et al. (2015) reported that hypoxia potentiates inflammation and glycolysis mostly through hexokinase II and ubiquitous 6-phosphofructo-2-kinase (PFKFB3) pathways associated with cell viability (Tawakol et al. 2015). Additionally, glycolytic rate is dependent on the cellular concentration of fructose 2,6-bisphosphate (Fru-2,6-P2), and that is controlled by PFK-2. Another rate-limiting enzyme of glycolysis is phosphofructokinase-1 (PFK-1), which is activated by Fru-2,6-P2, and overrides the inhibitory effect of ATP on PFK-1 (Calvo et al. 2006; Van Schaftingen et al. 1981). On the other hand, the expression of PFKFB3 is high in cancer cells and controlled by phosphatase and tensin homolog (PTEN) and PI3K/Akt pathways, which required for cell cycle progression and prevention of apoptosis may be partly due to the ability of F2,6BP to activate cell cycle markers cyclin-dependent kinases (CDKs) (Yalcin et al. 2014). Interestingly, much about the basic metabolomics abnormalities in keratinocytes remains poorly understood in CEES challenge. Hence, in the present study, the aim is to determine the CEES-induced oxidative-nitrosative stress–mediated alteration of Erk1/2 and PI3K/Akt, antioxidant depletion, and changes in metabolites, leading to biomolecule damage, inflammation and loss of cell–cell communication trigger cell cycle deregulation and apoptosis. We also demonstrated that pretreatment of pharmacological inhibitors like *N*-acetyl cysteine (NAC), L-Nω-nitroarginine methyl ester (NAME), hydralazine hydrochloride (Hyd·HCl), LY294002 (Ly), Wortmannin (Wt), PD98059 (U1), and U0126 (U2) counteracts the effects of CEES in keratinocytes.

Materials and methods

Reagents and antibodies

Fetal bovine serum (FBS) and Dulbecco's modified eagle medium (DMEM) were purchased from GIBCO (Invitrogen, USA). Dihydroethidium (DHE) and dihydrorhodamine 123 (DHR) were purchased from Molecular probes (Eugene, OR). Propidium iodide (PI), 3-(4,5-dimethylthiazol-2-yl)-2,5-diphenyltetrazolium bromide (MTT), NAC, Hyd·HCl, NAME, and inhibitors of PI3K/Akt (Ly, Wt) were purchased from Sigma-Aldrich, USA. Neutral red was purchased from Himedia, India. Antibodies against phospho- and total-Erk1/2, Akt, tuberin, mTOR, chk1, chk2, caspases, β-tubulin, horseradish peroxidase (HRP)–conjugated secondary antibodies, and inhibitors of Erk1/2 (U1, U2) were purchased from Cell Signaling Technology, USA.

Animals and experimental design

SKH-1 hairless mice (6 weeks age) were obtained from Charles River Laboratories (Wilmington, MA, USA) and housed under standard conditions at the Center for Laboratory Animal Care, School of Biotechnology, KIIT. For the animal experiments, we followed the protocol described by Tewari-Singh et al. (2009). Specified protocol was approved by animal ethics approval at the School of Biotechnology, KIIT. Freshly prepared acetone alone or different concentrations of CEES diluted in acetone were applied topically on the dorsal surface of mice skin in a continuously operated biological safety fume hood. In the dose-dependent study, mice were exposed to CEES ranging from 1 to 2 mg in 200 μl acetone per mouse that was applied on the dorsal skin along with mice taken as control (C) and vehicle control (VC, 200 μl acetone alone per mouse) for 12 h. At the end of experiment time, the mice were euthanized, and the dorsal skin was collected and snaps frozen in liquid nitrogen and transferred to deep freezer as described in our previous study (Pal et al. 2009).

Cell culture and treatments

Mouse keratinocyte (JB6) cells were obtained as a kind gift from Prof. Rajesh Agarwal, Department of Pharmaceutical Sciences, University of Colorado Denver, USA. Human skin keratinocytes, HaCaT cells, were obtained from NCCS Pune, India. Cells were grown in low-glucose (5 mM) DMEM for JB6 cells, and DMEM with Nutrient Mixture F-12 Ham medium for HaCaT cells in the presence of 10% FBS in 37 °C humidified incubator. After getting 70–80% confluency in different plates such as 96-well plates, 6-well plates, 60-mm plates, and 100-mm plates as per the experimental requirement, cells were exposed to different concentrations of CEES (50, 100, 250, 500, and 1000 μM) with/without inhibitors for 24 h.

Measurement of RNS and ROS

RNS generation was determined by NO production by measuring the nitrite using Griess reagent (Yoo et al. 2005). Briefly, equal volume of culture media and Griess reagent (100 μl each) were mixed together and the absorbance was monitored at 540 nm. Intracellular production of ONOO– and O2·– was measured by using the DHR and DHE dyes respectively (Cury-Boaventura and Curi 2005). Cells were cultured in the presence or absence of CEES with/without inhibitors. After 24 h, cells were harvested and washed with phosphate-buffered saline (PBS) followed by staining with 5 μM DHR or DHE dyes separately for 30 min. Subsequently, the positive or negative fluorescence staining of cells was measured by a fluorescence-activated cell sorting (FACScan) analyzer with CELL Quest software (BD Bioscience, USA). For microscopic analysis, cells were seeded onto glass cover slips with/without inhibitors in the presence or absence of CEES. After 24 h, cells were harvested, washed with PBS, fixed with 3.7% paraformaldehyde, and stained with same dyes. Thereafter, the glass coverslip was mounted onto a glass slide and observed under microscope (BX61, USA). The hydroxyl radical (·OH) level was determined as described previously (Kumar et al. 2016). Briefly, treated cells were harvested and 300 μL (80 g protein) lysate was mixed with 700 μL of PBS solutions (0.1 M EDTA, 2 mM sodium salicylate, 40 μL 10 N HCl, and 0.25 g NaCl). Equal volume of ice cold diethyl ether was added, incubated for 30 min at 25 °C, and absorbance was recorded at 510 nm.

Measurement of antioxidants

The CAT activity in cell lysate was measured by spectrophotometer as described earlier (Kumar et al. 2016). Briefly, 80 μg of protein sample was dissolved in 800 μl of 50 μM phosphate buffers and 400 μl of 30 μM hydrogen peroxide (H_2O_2) and mixed immediately before absorbed rate kinetic at 240 nm. For the measurement of GSH, we followed the protocol described earlier (Manikandan et al. 2010). Briefly, cells were lysed in 0.2% Triton X-100 with PBS then homogenized and centrifuged at 15000 g. First, we prepared a reaction mixture (0.02 M EDTA, 50% trichloroacetic acid, Tris buffer, pH 8.8), and 500 μl of this solution was mixed with 100 μl of 2,4-dinitrophenylhydrazine (DNPH) and 80-μg protein samples incubated at 37 °C and obtained absorbance at 412 nm.

Measurement of biomolecule damage

For the measurement of LPO, a reaction mixture was prepared as described in earlier protocol (Sagar et al. 2017), mixed with 100 μl of protein samples (80 μg) and incubated in 37 °C for 1 h. Thiobarbituric acid (0.375%) was then added to the reaction mixture and allowed to react at boiling water bath for 15 min, followed by centrifugation at 800 g and the absorbance was measured at 532 nm. For the PC measurement, 450 μl of protein sample (80 μg) was mixed with 450 μl of buffer (Sagar et al. 2017) and 100 μl of 10% streptomycin sulfate, mixed thoroughly, and centrifuged at 1000 g. Next, 400 μl of the above supernatant was mixed with 400 μl of 10 mM DNPH, and kept in the dark. Thereafter, 20% ice-cold trichloroacetic acid was added to each sample to stop the reaction and centrifuged at 1000 g. Protein pellet from each tube was carefully washed with 2 ml of absolute ethanol: ethyl acetate solution. The final pellet was dissolved in 1 ml of guanidine hydrochloride (6 M) and absorbance was recorded at 366 nm.

Cell viability, apoptosis, and cell cycle analysis

The MTT assay was carried out as described earlier (Stone et al. 2003). Briefly, cells were cultured in 96-well plates and in the following day, cell were exposed with various concentrations of CEES for 12 h (JB6 cells) and 24 h (HaCaT cells) with/without inhibitors as indicated above. Subsequently, the treatment-containing medium was removed and MTT was added in each well of the plates. After 4 h, purple formazan product was dissolved by adding DMSO. The absorbance of the resulting solutions was measured at 570 nm using a microplate reader (Bio-Tek, USA). For the cell cycle analysis, treated cells were washed in PBS, pelleted, and resuspended in PI solution and fluorescence was measured on a FACS analyzer (Wang and Youle 2009). For the measurement of apoptotic cell, treated cells were harvested and resuspended in binding buffer. Thereafter, 100 μL of the cell suspension was mixed with 5 μL of annexin V–fluorescein isothiocyanate (FITC) (BD Pharmingen, CA) and 2 μL of PI. After 15 min of incubation, the cells were diluted with 300 μL of binding buffer. Fluorescent signals of FITC and PI were detected by a FACSan.

Lysosomal staining

Lysosomal staining was carried out as described earlier (Mytych et al. 2016). Briefly, after desired treatment as indicated above, Neutral Red (0.001%) was added and incubated at 37 °C for 3 h. The cells were fixed in formaldehyde (0.5%) in 1% $CaCl_2$ solution for 20 min, washed with water, and examined under fluorescence microscope (FLoid Cell Imaging Station, Grand Island, USA).

Western blotting

Cells were harvested after desired treatment as indicated above and lysed with lysis buffer (Pal et al. 2009), and protein concentration in the resulting lysate was determined using Bradford assay. Equal amounts of protein from the desired samples (40–50 μg) were resolved by electrophoresis in 8 to 12% Tris-glycine polyacrylamide gels, transferred to nitrocellulose membranes and incubated in blocking solution. Membranes were incubated overnight with the primary antibodies followed by corresponding secondary antibodies. The membranes were washed and the bound secondary antibody was detected using an enhanced chemiluminescence (ECLTM plus, Amersham). The same membrane was reprobed with anti-β-tubulin antibody as loading control.

6-Phosphofructo-2-kinase activity assay

Cells were harvested after desired treatment in 60-mm plates as indicated above and homogenized in 1 ml of medium containing 20 mM potassium phosphate (pH 7.4), 1 mM DTT, 50 mM NaF, 0.5 phenylmethanesulfonyl fluoride, 10 mM leupeptin, and 5% poly(ethylene)glycol. After centrifugation, poly(ethylene)glycol was added to the supernatant up to 15% (*w*/*v*) to fully precipitate the PFK-2. Subsequently, resuspension of the pellet in extraction medium, PFK-2 activity was assayed at pH 8.5, 5 mM fructose-6-phosphate, and 15 mM glucose-6-phosphate. One unit of PFK-2 activity is the amount of enzyme that catalyzes the formation of 1 pmol Fru-2,6-bisphosphate (Fru-2,6-P2)/min (Rodríguez-Prados et al. 2010).

RNA isolation and cDNA preparation

For RNA extraction, JB6 cells and mice skin tissues were harvested after desired treatment as indicated above and dissolved in Trizol (GIBCO). Then 200 μl of chloroform was added per milliliter of Trizol, mixed vigorously, and incubated for 10 min. Thereafter, samples were centrifuged and the upper layer of supernatant was transferred in a fresh tube. Further, isopropanol was mixed with supernatant and centrifuged and pellets were washed with ethanol. The concentration and purity of RNA was assessed using a NanoDrop ND-1000 Spectrophotometer (Epoch, USA). Reverse transcription was performed using the Revertaid First Strand cDNA Synthesis Kit (Thermo Scientific, Lithuania) according to the manufacturer's instructions, using oligo dT primers.

Quantitative real-time PCR

For quantification of mRNA, total RNA from tissues or cells were isolated using the HiPurA™Total RNA purification kit (Hi-media, India) and cDNA was prepared using Revert Aid cDNA synthesis kit (Thermo Scientific). Quantitative real-time PCR was performed with a CFX connect real-time system (BIO-RAD, USA) using the KAPA SYBR® FAST qPCR Kit (KAPA Biosystems). $2^{-\Delta\Delta CT}$ method was used to quantify relative levels of target genes using oligonucleotides (Table S1).

Measurement of thiol amino acid metabolites

Thiol (–SH) content was measured by a spectrophotometric method based on the reductive cleavage of 5-5′-dithiobis-(2-nitrobenzoic acid), and DTNB (Ellman 1959). The 5% (*w*/*v*) homogenate of cells and tissue lysates was prepared in 2.5% sulfosalicylic acid and was centrifuged at 10,000*g* for 10 min. Subsequently, 150 μl aliquots of supernatants were mixed with 800 μl of 0.1 M potassium phosphate buffer (pH 8.0) containing 1 mM EDTA, and 50 μl of DTNB (1 mg/ml). The absorbance of the resultant yellow color was measured at 412 nm. For each mole of –SH bound to DTNB, one mole of nitrobenzoate was released, which absorbs maximally at 412 nm. Total Cys content was estimated in mice and JB6 cells as described earlier (Wright and Viola 1998). The 5% (*w*/*v*) homogenate of cells and tissue lysate was prepared in 2.5% ice-cold perchloric acid and was centrifuged at 10,000*g* for 10 min. An acid ninhydrin reagent was prepared by dissolving 250 mg of ninhydrin in a mixture of 6 ml of acetic acid and 4 ml of concentrated hydrochloric acid. Clear solution was obtained by mixing for 20–30 min at room temperature. The Cys standards of the range 0.5–10 μg/ml were prepared by dissolving Cys in 10% perchloric acid. 0.5 ml of standard/sample was mixed with 0.5 ml of acetic acid and 0.5 ml of acid ninhydrin reagent. After thorough mixing, the tubes were covered and heated in water bath for 10 min at 100 °C. After cooling for 5 min on ice, 0.5 ml of cold ethanol (95%) was added to stabilize the pink color. Absorbance was recorded at 560 nm.

Data analysis and statistics

All the statistical analyses were performed using GraphPad Prism 5.0. Both one-way and two-way analysis of variance (ANOVA) were used to evaluate the significance between the groups followed by Student's *t* test. One-way ANOVA was used in both in vivo and in vitro experiments, to compare in between control, and treated groups in the case of in vivo experiments and control, and treated groups with/without inhibitors in the case of in vitro experiments, whereas two-way ANOVA was used specifically to compare the RT-PCR results both in animal and in cell culture experiments. A significance level of $P < 0.05$ was considered to be statistically significant. All experiments were performed 3–4 times and expressed as the mean ± standard error of the mean (SEM).

Results

CEES exposure augments NO and ONOO– production via iNOS is associated with Erk1/2 and Akt pathway in keratinocytes

We hypothesized that the stress signaling cascades have linked to oxidative stress pathway via phosphorylation of Erk11/2 and Akt after CEES exposure. As shown in Fig. 1a, the phosphorylation of Erk11/2 and Akt was increased after exposure of CEES in mice skin tissues without altering total protein levels. A similar kind of trend was observed in HaCaT cells treated with increasing concentration of CEES for 24 h (Fig. 1a). On the other hand, the isoform of nitric oxide synthase (iNOS) is expressed in almost all cell types including keratinocytes after stress that stimulate a large amount of NO production (Stone et al. 2003; Hasarmeh et al. 2016; Kim et al. 2006). Persistent with the above findings, we observed that the mRNA expression of iNOS was increased in 1.5 mg CEES exposure in mice skin tissues (Fig. 1b). Also, treatment of 500 μM CEES to keratinocytes cells for 24 h increased the iNOS mRNA expression and the increased expression of iNOS was attenuated by Erk11/2 or Akt inhibitors in keratinocyte cells (Fig. 1c). We also studied the effect of CEES on the NO production in keratinocytes. As shown in Fig. S1A, the NO production was increased with increasing concentration of CEES. For the time kinetic study, 500 μM CEES for different time points, the NO productions was also increased with time (Fig. S1b), while keratinocyte cells treated with NAC or NAME attenuated the NO production in the presence of CEES for 24 h (Fig. 1d). Thereafter, to understand whether NO is the downstream target of Erk1/2 and Akt, we exposed cells in the presence of Erk1/2 and PI3K/Akt inhibitors with/without CEES. As shown in Fig. 1e and f, both Erk1/2 and Akt inhibitors attenuated the NO production in the presence of CEES. To explore whether the product of the diffusion controlled the reaction of NO with O2·– is a short-lived oxidant species ONOO–, we studied the percent of ONOO–-positive cells cultured in CEES (Fig. S1c). To confirm the increase in ONOO–-positive cells after CEES exposure, keratinocyte cells were exposed with ONOO– inhibitor, Hyd·HCl. A decrease in ONOO– accumulation was observed in the presence of Hyd·HCl in HaCaT cells for 24 h (Fig. 1g and h). Further, to confirm that the ONOO– accumulation is due to Erk1/2 or Akt signaling pathways, we treated HaCaT cells with Erk1/2 or Akt inhibitors in the presence of CEES for 24 h. As shown in Fig. 1i and j, accumulated ONOO– in the presence of CEES was attenuated by both the inhibitors.

CEES exposure augments O2·– and ·OH production via Erk1/2 and Akt pathways in keratinocytes

From the above findings, we observed that CEES exposure augments NO production that leads to increase in ONOO– accumulation in keratinocytes. Further, to explore the product of the diffusion-controlled reaction of NO with O2·– is a short-lived oxidant species ONOO–, we measured O2·– in CEES-treated animal and cell culture models. As shown in Fig. 2a, an increased O2·– production was observed with exposure to increasing concentrations of CEES to SKH-1 hairless mice skin. A similar kind of trend was observed in keratinocyte cells treated with increasing concentration of CEES (Fig. S2a&b) and 500 μM CEES for different time points (Fig. S2c). In the treatment of cells with ROS inhibitor, NAC attenuated the CEES-induced O2·– accumulation in keratinocyte cells (Fig. 2b). We also checked with Erk1/2 and Akt inhibitors whether the O2·– production was augmented by CEES via Erk1/2/Akt pathway or not. As shown in Fig. 2c and d, pretreatment of cells with Erk1/2 or Akt inhibitors attenuated CEES-induced O2·– production in keratinocyte cells. As evidenced by NBT, a major marker of O2·– was significantly enhanced 1.5–2-folds as compared to control cells upon the CEES treatment. To further

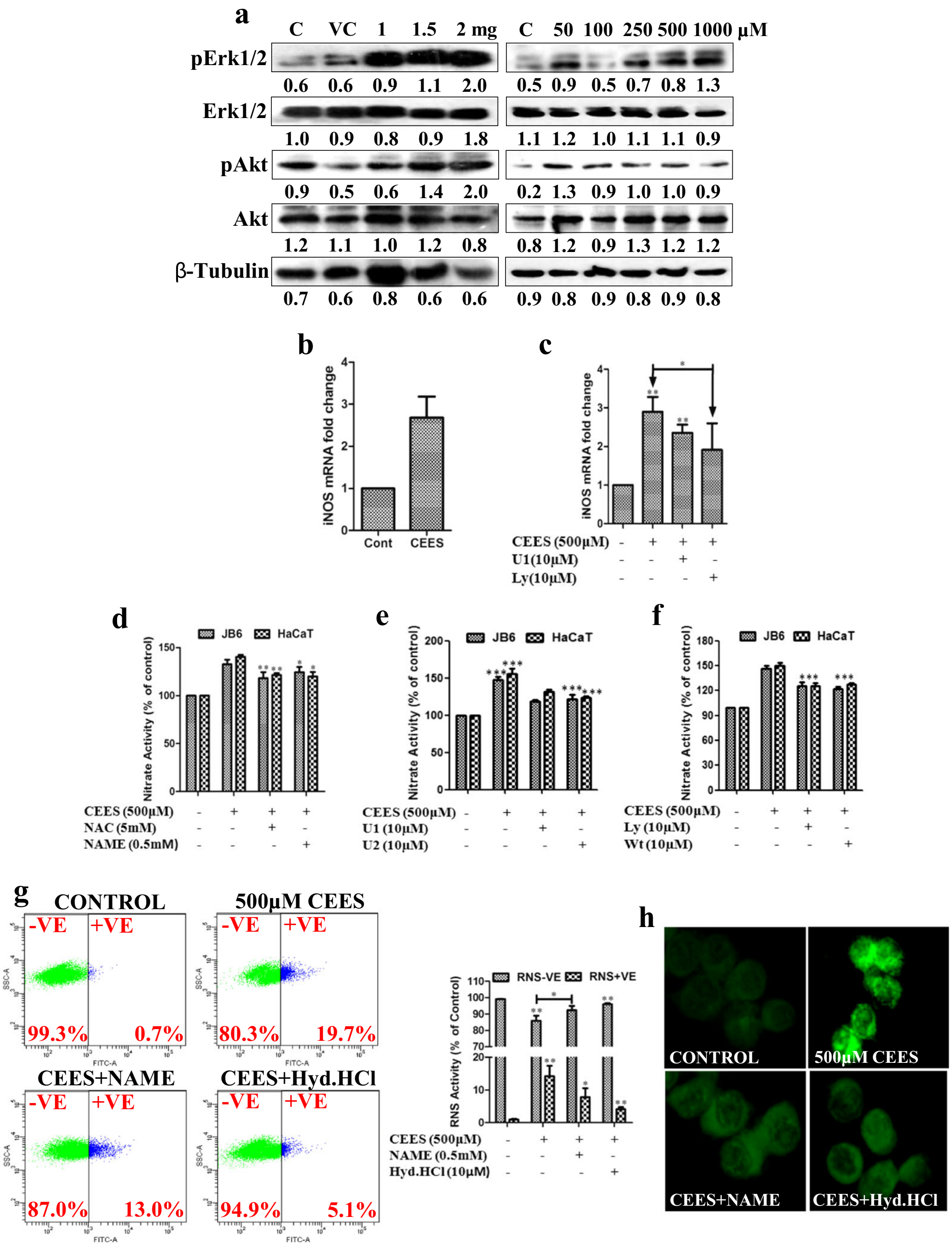

Fig. 1 CEES exposure augments RNS production which is associated with the Erk11/2-Akt pathway in keratinocytes. A representative immunoblot of Erk11/2 and Akt in SKH-1 hairless mice skin tissues and in HaCaT cells with increasing dose of CEES (**a**). qRT-PCR analysis showing iNOS expression in SKH-1 hairless mice skin tissues (**b**) and in HaCaT cells with 500 µM CEES in the presence or absence of Erk11/2 or Akt inhibitors (**c**). Spectrophotometer assay showing NO generation in keratinocyte cells in the presence of 500 µM CEES with or without NAC, and NAME (**d**), and Erk11/2 (**e**) or Akt inhibitors (**f**). A representative FACS analysis of ONOO—-positive cells cultured in 500 µM CEES with or without NAME or Hyd·HCl (**g**), and fluorescent microscopic image of ONOO—-positive cells cultured in 500 µM CEES with or without NAME or Hyd·HCl (**h**). A representative FACS analysis of ONOO—-positive cells cultured in 500 µM CEES with or without Erk11/2 or Akt inhibitors (**i**), and fluorescent microscopic image of ONOO—-positive cells cultured in 500 µM CEES with or without Erk11/2 or Akt inhibitors (**j**). (***$p < 0.001$, **$p < 0.01$, and *$p < 0.05$)

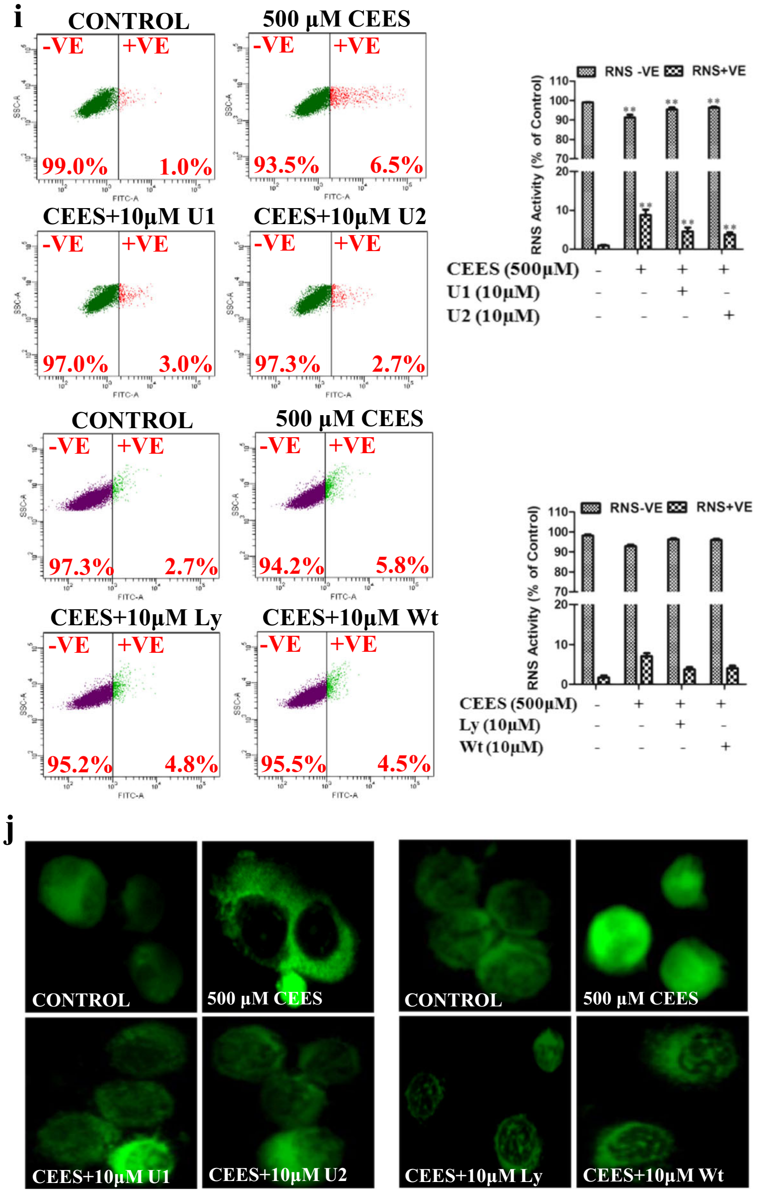

Fig. 1 (continued)

confirm the O2·–generation was augmented by CEES exposure, we measured the O2·–-positive cells by FACS and microscopy techniques. Both the analysis established that CEES exposure augmented O2·– production in keratinocyte cells and pretreatment of cells with ROS inhibitor, NAC, or Erk1/2 or Akt inhibitors attenuated CEES-induced O2·– production in keratinocyte cells (Fig. 2e–g). Subsequently, we measured the CEES-induced ·OH production, another ROS marker in keratinocyte cells. As shown in Fig. 2h, the ·OH production was increased with increasing concentration of CEES in mice skin tissues. A similar kind of trend was observed in keratinocyte cells treated with increasing concentration of CEES and 500 µM CEES for different time points (Fig. S2d&e). While HaCaT cells were treated with NAC, it attenuated the ·OH production in the presence of CEES for 24 h (Fig. 2i). Thereafter, to understand whether ·OH is the downstream target of Erk1/2 and Akt, we exposed cells with Erk1/2 or PI3K/Akt inhibitors in the presence or absence of CEES for 24 h. As shown in Fig. 2j and k, Erk1/2

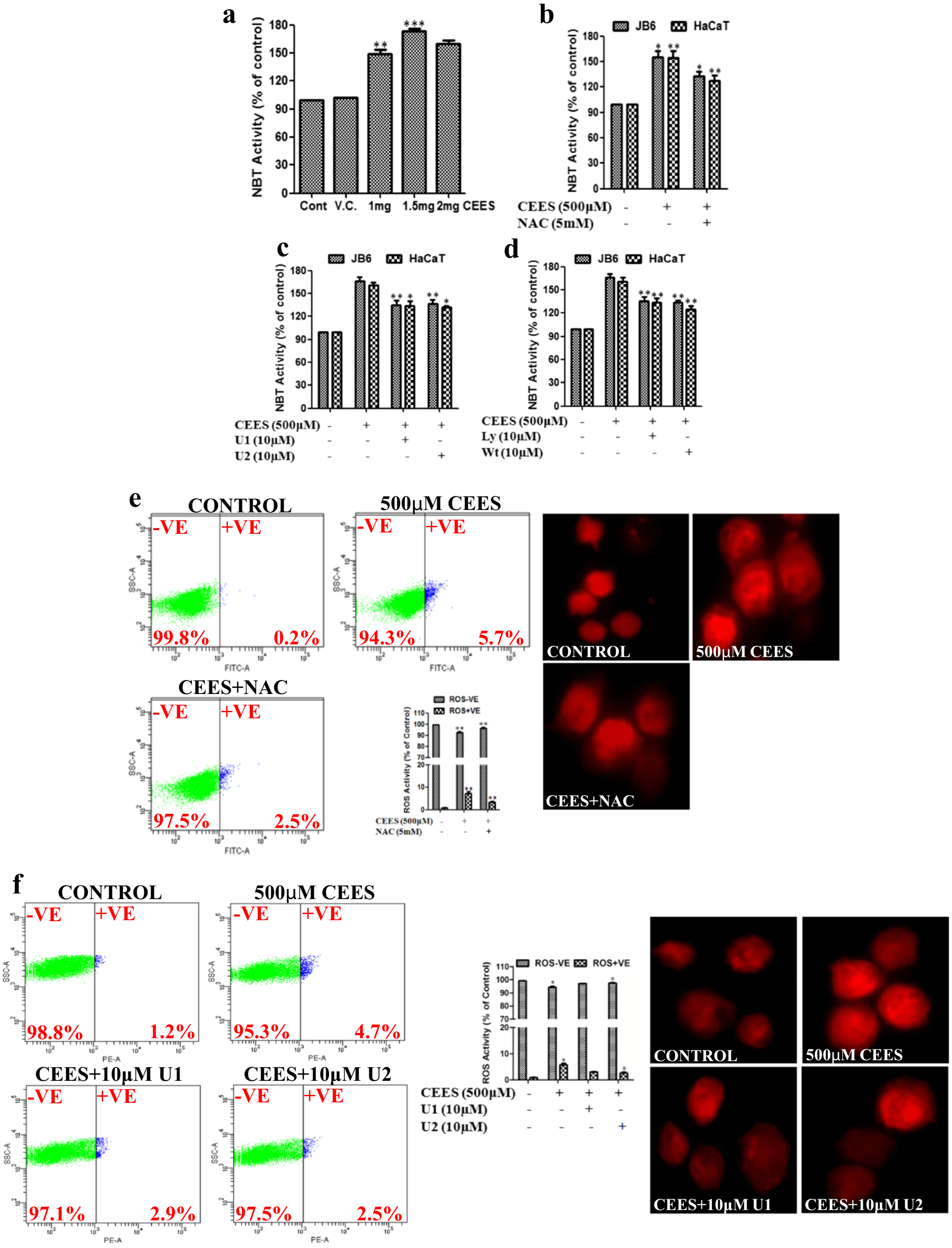

Fig. 2 CEES exposure augments ROS production via Erk11/2 and Akt pathway in keratinocytes. NBT assay showing O2·– production in SKH-1 hairless mice skin with exposure to increasing concentrations of CEES (**a**). Pretreatment of NAC (**b**) or Erk11/2 (**c**) or Akt (**d**) inhibitors attenuated the CEES (500 µM)-induced O2·– production in HaCaT cells. A representative FACS analysis of O2·–-positive cells (**e**, left panel), and fluorescent microscopic image of O2·–-positive cells (**e**, right panel) cultured in 500 µM CEES with or without NAC. A representative FACS analysis of O2·–-positive cells and fluorescent microscopic image of O2·–-positive cells cultured in 500 µM CEES with or without Erk11/2 (**f**) or Akt inhibitors (**g**). Spectrophotometer assay showing ·OH production in SKH-1 hairless mice skin with exposure to increasing concentrations of CEES (**h**). Pretreatment of NAC (**i**) or Erk11/2 (**j**) or Akt (**k**) inhibitors attenuated the CEES (500 µM)-induced ·OH production in HaCaT cells. (***$p < 0.001$, **$p < 0.01$, and *$p < 0.05$)

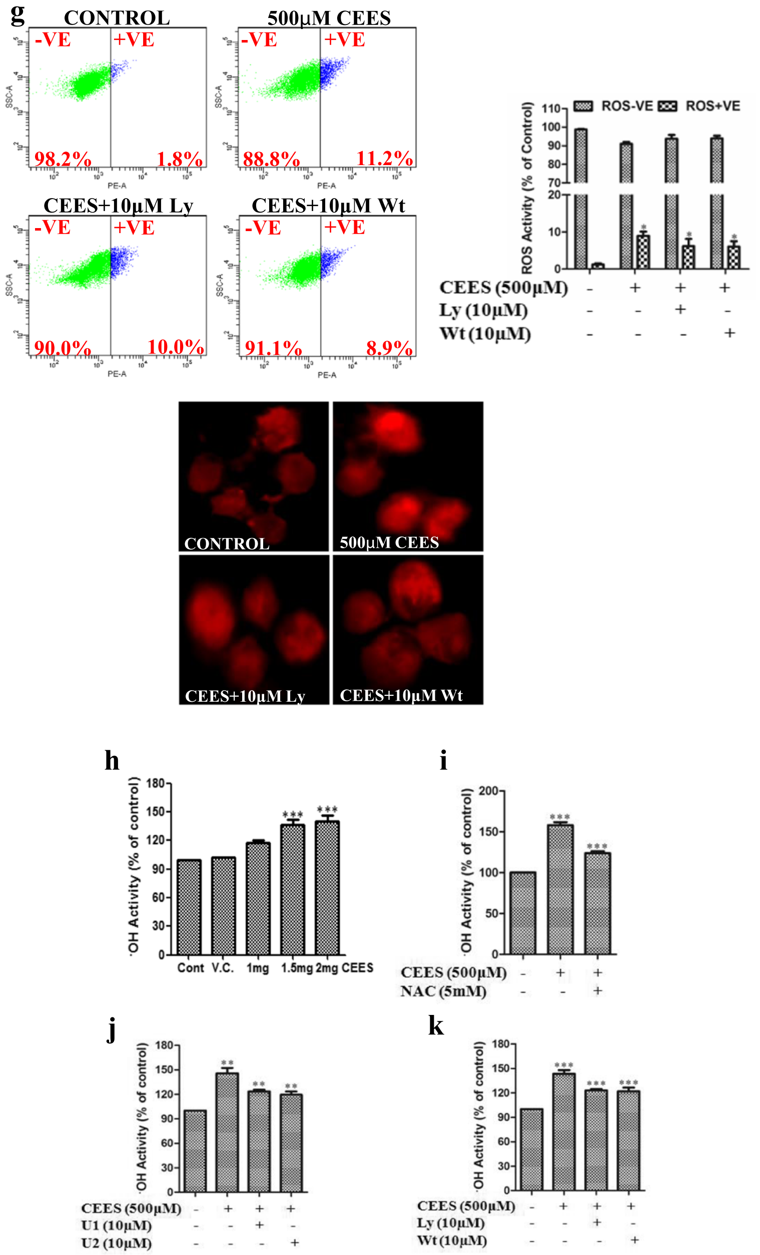

Fig. 2 (continued)

or Akt inhibitors attenuated the ·OH production in the presence of CEES in HaCaT cells.

CEES exposure augments oxidative stress which trigger depletion of antioxidant capacity via Erk1/2-Akt pathway in keratinocytes

Cellular antioxidant activities such as CAT, GSH, and GPx in SKH-1 mice, and keratinocyte cells subjected to CEES exposure, decreased with increasing concentrations of CEES (Fig. 3a). A similar kind of trend was observed in keratinocyte cells treated with increasing concentration of CEES (Fig. S3a) and 500 μM CEES for different time points (Fig. S3b). To further confirm that the CEES effect was mediated by ROS and RNS production, keratinocyte cells were pretreated with NAC or NAME or Hyd·HCl before CEES exposure and then antioxidant levels were investigated. We

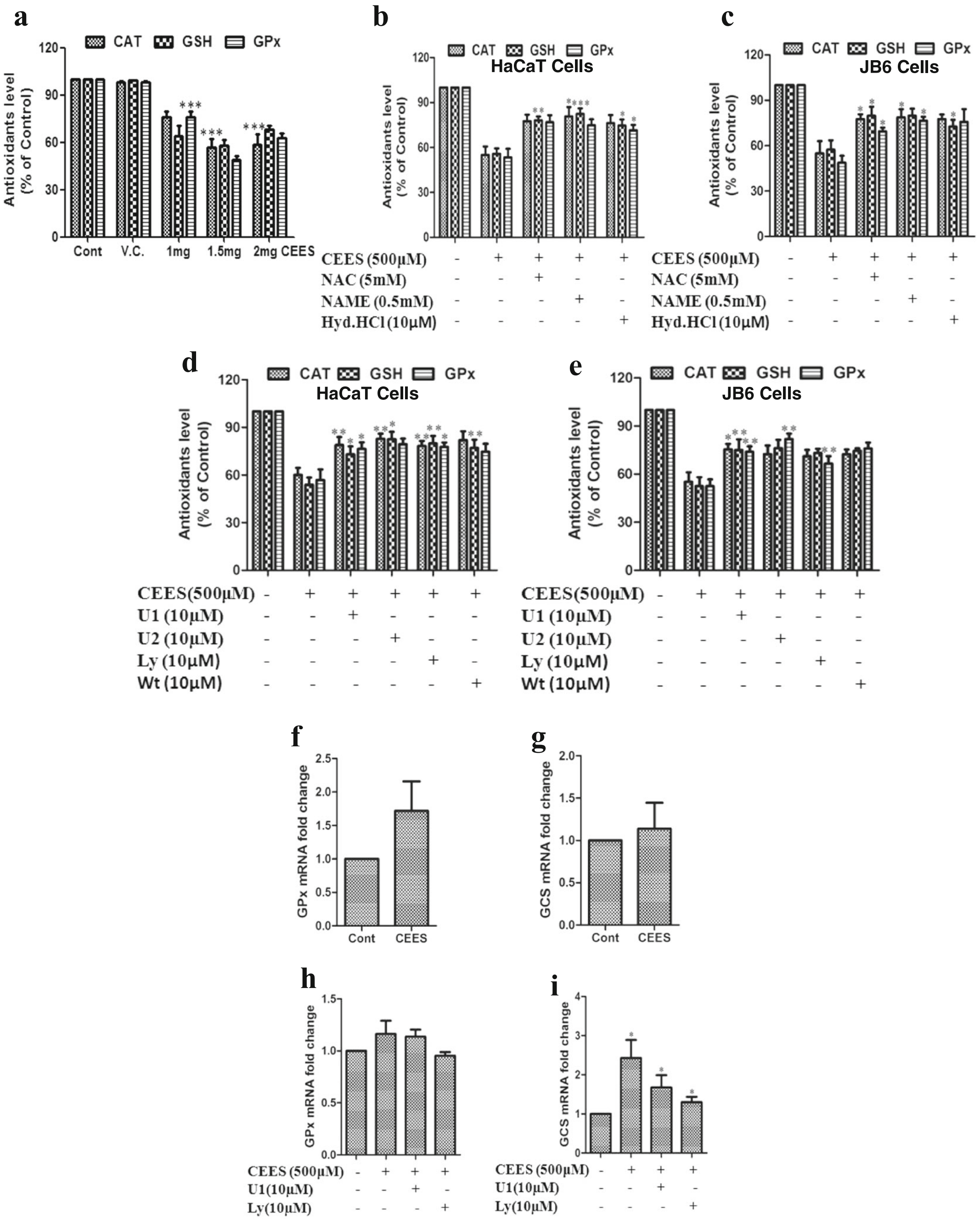

Fig. 3 CEES exposure augments oxidative stress which triggers depletion of antioxidant capacity via Erk11/2-Akt pathway in keratinocytes. Spectrophotometer assay showing decrease in antioxidants such as CAT, GSH, and GPx in SKH-1 hairless mice skin with exposure to increasing concentrations of CEES (a). Pretreatment of NAC or NAME or Hyd·HCl (b and c) or Erk11/2 or Akt inhibitors attenuated the CEES (500 µM)-induced O2·– production in HaCaT (d) and JB6 (e) cells. QRT-PCR analysis of GPx (f) and GCS (g) in mice skin tissues treated with 1.5 mg CEES. Pretreatment of Erk11/2 (h) or Akt (i) inhibitors attenuates the GPx and GCS mRNA expression in HaCaT cells in the presence of 500 µM CEES. (***$p < 0.001$, **$p < 0.01$, and *$p < 0.05$)

observed that antioxidant levels were improved within 24 h in a dose-dependent treatment of inhibitors (Fig. 3b and c). Further, we checked with Erk1/2 or Akt inhibitors whether the depletion of antioxidant capacity regulated by CEES induced oxidative stress via Erk1/2/Akt pathway or not. As shown in Fig. 3d and e,

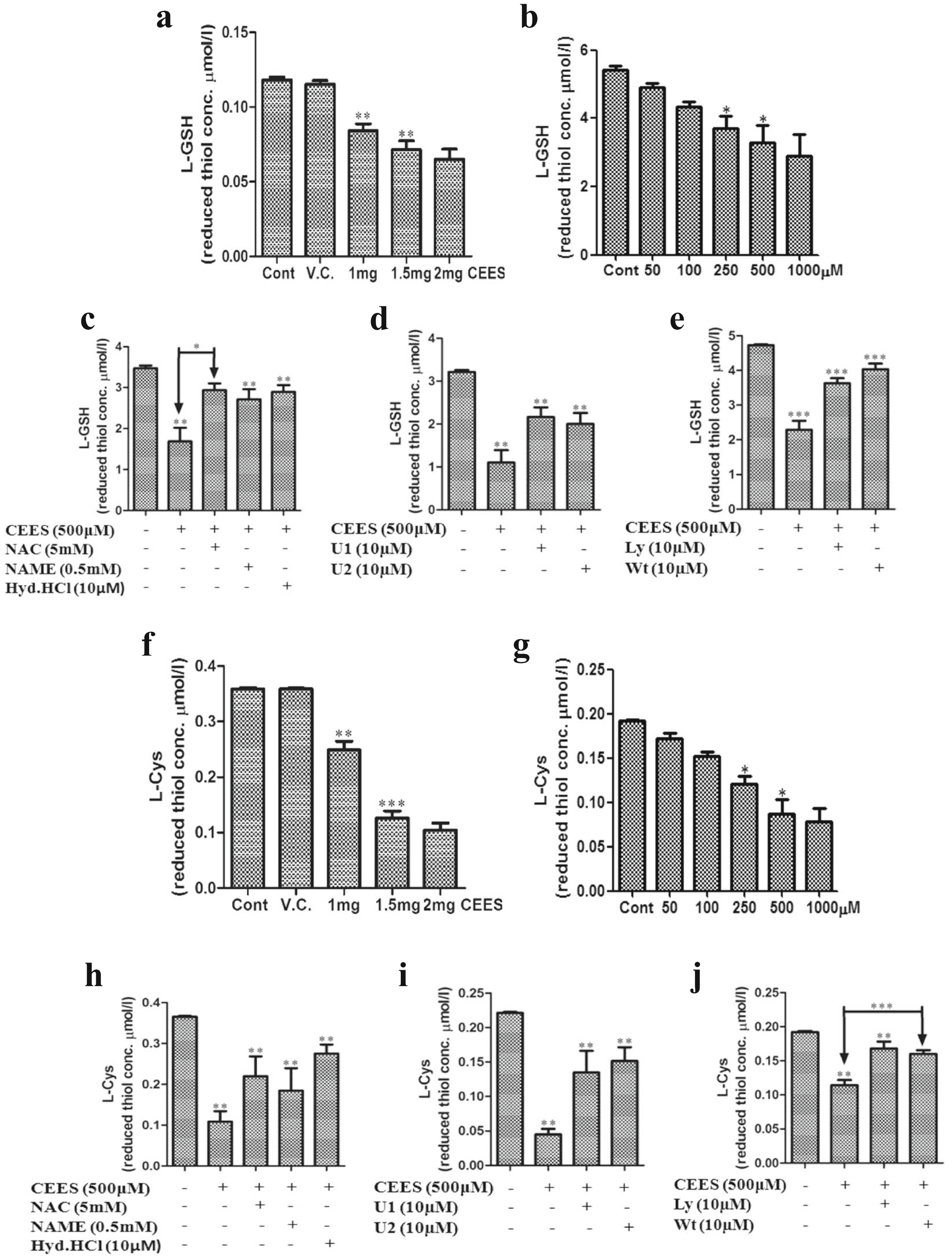

Fig. 4 CEES exposure augments oxidative stress which triggers depletion of thiol amino acid metabolites via Erk11/2-Akt pathway in keratinocytes. Spectrophotometer assay showing decrease in L-GSH amino acid metabolites in SKH-1 hairless mice skin with exposure to increasing concentrations of CEES (**a**), and HaCaT cells treated with increasing concentration of CEES (**b**). Pretreatment of NAC or NAME or Hyd·HCl (**c**) or Erk11/2 (**d**) or Akt (**e**) inhibitors attenuated the CEES (500 µM) decrease in L-GSH amino acid metabolites in HaCaT cells. Spectrophotometer assay showing decrease in L-Cys amino acid metabolites in SKH-1 hairless mice skin with exposure to increasing concentrations of CEES (**f**), and HaCaT cells treated with increasing concentration of CEES (**g**). Pretreatment of NAC or NAME or Hyd·HCl (**h**) or Erk11/2 (**i**) or Akt (**j**) inhibitors attenuated the CEES (500 µM) decrease in L-Cys amino acid metabolites in HaCaT cells. (***$p < 0.001$, **$p < 0.01$, and *$p < 0.05$)

pretreatment of cells with Erk1/2 or Akt inhibitors attenuated CEES-induced depletion of antioxidants in keratinocyte cells. Subsequently, we checked the GPx and GCS levels by qRT-PCR in both mice and JB6 cells. As shown in Fig. 3f and g, the mRNA expression of GPx and GCS was increased in 1.5 mg CEES exposure to mice skin. Similarly, CEES exposure to HaCaT cells increases the mRNA expression of GPx and GCS in the presence of 500 μM CEES for 24 h and pretreatment of Erk1/2 or Akt inhibitors attenuates the GPx and GCS mRNA expression (Fig. 3h and i).

CEES exposure augments oxidative stress which triggers depletion of thiol amino acid metabolites via Erk1/2-Akt pathway in keratinocytes

The increase in ROS/RNS production and depletion of cellular antioxidants specifically GSH causes the S-glutathiolation of the critical Cys residue in the propeptide domain that disrupts its binding to the catalytic Zn2+ ion, resulting in an active full length enzyme in cellular compartments. To measure the thiol amino acid metabolite depletion such as L-GSH and L-Cys, after CEES exposure with NAC or NAME or Hyd·HCl or Erk1/2 or Akt inhibitors, we assayed spectrophotometrically in animal and cell culture models. As shown in Fig. 4a, a decreased L-GSH level was observed with exposure to increasing concentrations of CEES as compared with the control mice. A similar kind of trend was observed in HaCaT cells treated with increasing concentration of CEES for 24 h (Fig. 4b). We also checked with NAC or NAME or Hyd·HCl or Erk1/2 or Akt inhibitors whether the depletion of L-GSH is augmented by CEES via oxidative stress or Erk1/2-Akt pathway or not. Treatment of cells with inhibitors for 24 h attenuated the CEES-induced depletion of L-GSH in HaCaT cells (Fig. 4c–e). Next, we measured L-Cys treated with CEES both in vitro and in vivo models. As shown in Fig. 4f, a decreased L-Cys level was observed with exposure to increasing concentrations of CEES as compared with the control mice. A similar kind of trend was observed in HaCaT cells treated with increasing concentration of CEES for 24 h (Fig. 4g). Pretreatment of cells with NAC or NAME or Hyd·HCl or Erk1/2 or Akt inhibitors for 24 h attenuated CEES-induced depletion of L-Cys in HaCaT cells (Fig. 4h–j).

CEES exposure augments oxidative stress which triggers alteration of PFK-2 proteins via Erk1/2-Akt pathway in keratinocytes

Recently, studies have shown that under stress conditions, PFKFB3 levels were high and the expression PFKFB3 was controlled by MAPK pathway (Novellasdemunt et al. 2013). However, there are different genes that encode PFK-2 proteins such as PFKFB-1, PFKFB2, PFKFB3, and PFKFB4 (Rider et al. 2004). Treatment of mice with various doses of CEES strongly deactivates the PFK-2 protein (Fig. 5a). A similar kind of trend was observed in HaCaT cells treated with increasing concentration of CEES for 24 h (Fig. 5b). While keratinocyte cells were treated with NAC, it reversed the PFK-2 protein in the presence of CEES for 24 h (Fig. 5c). Thereafter, to understand whether PFK-2 is the downstream target of NO or ONOO–, we exposed cells with inhibitors of NAME or Hyd·HCl in the presence or absence of CEES for 24 h. As shown in Fig. 5d, NAME or Hyd·HCl reversed the PFK-2 protein depletion in the presence of CEES. Further, we checked with Erk1/2 or Akt inhibitors whether the increase of PFK-2 proteins is augmented by CEES via Erk1/2-Akt pathway or not. Treatment of HaCaT cells with Erk1/2 or Akt inhibitors for 24 h reversed the CEES-induced increase of PFK-2 proteins in HaCaT cells (Fig. 5e and f). Next, we checked the expression of PFK-2 isoform genes PFKFB-1, and PFKFB3. Treatment of mice with 1.5 mg CEES strongly activates PFKFB1 and PFKFB3 (Fig. 5g and h). To further characterize the response in HaCaT cells to the Erk1/2 or Akt inhibitors at metabolic level, there was an increase in the basal levels of PFKFB1 and PFKFB3, a potent activator of the glycolytic flux, and impaired its further decrease (Fig. 5i and j).

CEES exposure augments oxidative stress which triggers biomolecular damage and associated with loss of cell–cell communications via Erk1/2-Akt pathway in keratinocytes

Subsequently, we examined the LPO and PC by CEES treatment in animal and cell culture models. As shown in Fig. 6a, increased LPO and PC were observed in mice skin tissues with increasing concentrations of CEES exposure. Further, a similar kind of trend was observed in keratinocyte cells treated with increasing concentration of CEES (Fig. 6b and c). We also checked 500 μM

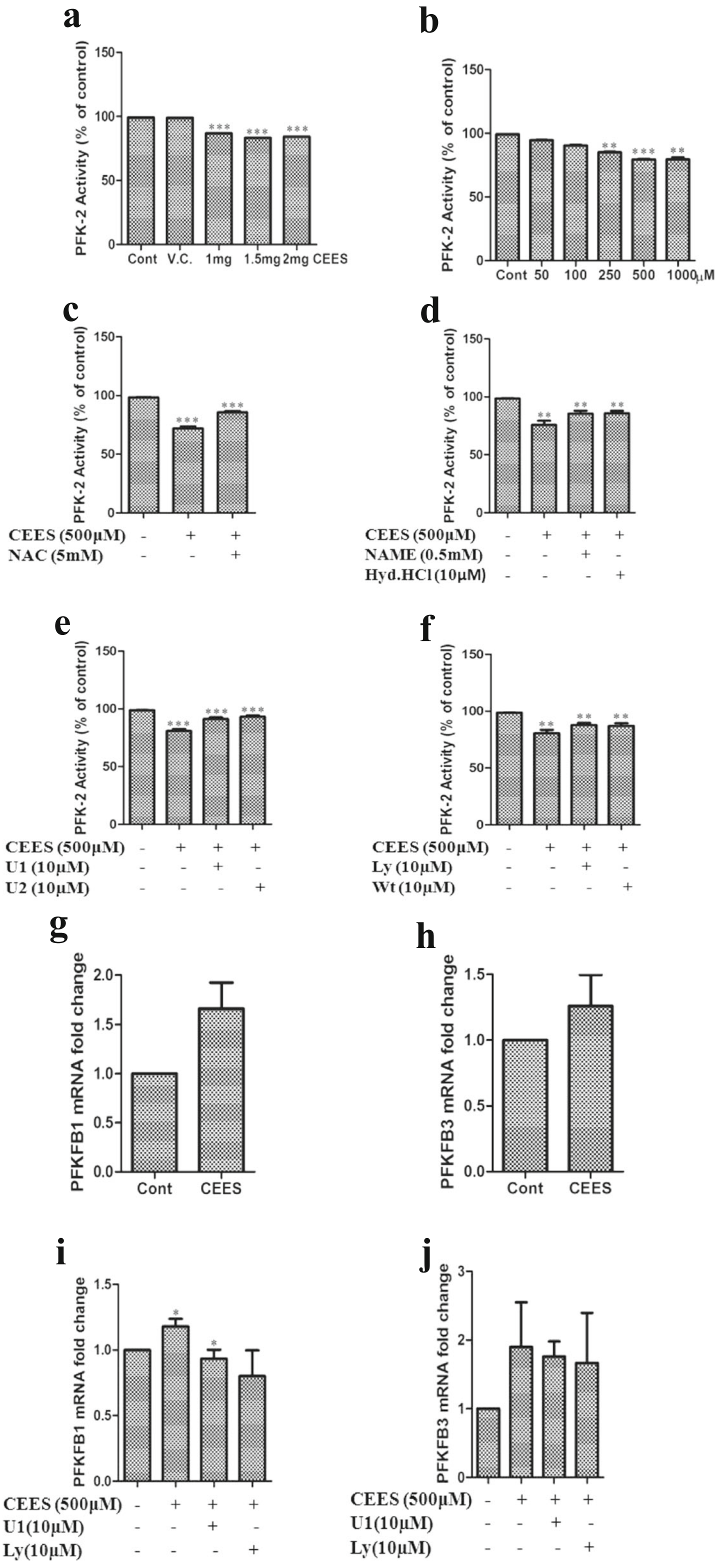
a
PFK-2 Activity (% of control)
150
100
50
0
***
***
***
Cont
V.C.
1mg
1.5mg
2mg CEES
b
PFK-2 Activity (% of control)
150
100
50
0
**
***
**
Cont
50
100
250
500
1000μM
c
PFK-2 Activity (% of control)
150
100
50
0
***
***
CEES (500μM) - + +
NAC (5mM) - - +
d
PFK-2 Activity (% of control)
150
100
50
0
**
**
**
CEES (500μM) - + + +
NAME (0.5mM) - - + -
Hyd.HCl (10μM) - - - +
e
PFK-2 Activity (% of control)
150
100
50
0
***
***
***
CEES (500μM) - + + +
U1 (10μM) - - + -
U2 (10μM) - - - +
f
PFK-2 Activity (% of control)
150
100
50
0
**
**
**
CEES (500μM) - + + +
Ly (10μM) - - + -
Wt (10μM) - - - +
g
PFKFB1 mRNA fold change
2.0
1.5
1.0
0.5
0.0
Cont
CEES
h
PFKFB3 mRNA fold change
1.5
1.0
0.5
0.0
Cont
CEES
i
PFKFB1 mRNA fold change
1.5
1.0
0.5
0.0
*
*
CEES (500μM) - + + +
U1(10μM) - - + -
Ly(10μM) - - - +
j
PFKFB3 mRNA fold change
3
2
1
0
CEES (500μM) - + + +
U1(10μM) - - + -
Ly(10μM) - - - +

◀ **Fig. 5** CEES exposure augments oxidative stress which triggers alteration of PFK-2 via Erk11/2-Akt pathway in keratinocytes. Spectrophotometer assay showing decrease in PFK-2 in SKH-1 hairless mice skin with exposure to increasing concentrations of CEES (**a**), and HaCaT cells treated with increasing concentration of CEES (**b**). Pretreatment of NAC (**c**) or NAME or Hyd·HCl (**d**) or Erk11/2 (**e**) or Akt (**f**) inhibitors attenuated the CEES (500 μM) decrease in PFK-2 in HaCaT cells. QRT-PCR analysis of PFKFB1 (**g**) and PFKFB3 (**h**) in mice skin tissues treated with 1.5 mg CEES. Pretreatment of Erk11/2 or Akt inhibitors attenuates the PFKFB1 (**i**) and PFKFB3 (**j**) mRNA expression in HaCaT cells in the presence of 500 μM CEES. (***$p < 0.001$, **$p < 0.01$, and *$p < 0.05$)

CEES for different time points and observed that LPO and PC increased with increasing duration of CEES treatment in both the keratinocyte cells (Fig. S4). Thereafter, we checked with pretreatment of NAC or NAME or Hyd•HCl inhibitors' presence or absence of CEES in keratinocyte cells. Treatment of cells with inhibitors attenuated the CEES-induced increase of LPO and PC in keratinocytes (Fig. 6d and e). To further confirm that the increase in LPO and PC after CEES exposure was mediated by Erk1/2 or Akt pathway, we used Erk1/2 or Akt inhibitors in keratinocyte cells. As shown in Fig. 6f and g, LPO and PC levels were reduced when pretreated with Erk1/2 or Akt inhibitors in the presence of 500 μM CEES. Protein and lipid damage in cellular membrane regions due to CEES exposure may directly affect the cell–cell communication by Gap junction (GJ) molecules present in keratinocytes. Gap junction channels consist of two hemichannels called connexons, each formed by six polypeptides belonging to a family of transmembrane proteins called connexions (Cx). Also, in keratinocytes, GJ has been hypothesized to be involved in the regulation of keratinocyte growth, differentiation, and migration. Connexins including Cx26, Cx32, and Cx43 play a key role in tissue homeostasis and were expressed during the keratinocyte differentiation process. Moreover, Pannexin (Panx)1 and Panx3 play key roles in epidermal keratinocyte differentiation. Hence, we checked the GJ involved in keratinocyte damage after CEES exposure. Treatment of mice with 1.5 mg CEES strongly reduced the expression of Cx26, Cx32, and Cx43, and Panx1 and Panx3 (Fig. 6h and i). A similar kind of trend was observed in HaCaT cells treated with increasing concentration of CEES for 24 h (data not shown). Thereafter, to understand whether GJ is the downstream target of Erk1/2 or Akt, we exposed cells with Erk1/2 or PI3K/Akt inhibitors in the presence or absence of CEES for 24 h. As shown in Fig. 6j and k, both Erk1/2 and Akt inhibitors attenuated the expression of GJ molecules in the presence of CEES.

CEES exposure augments oxidative stress which triggers expression of inflammatory mediators via Erk1/2-Akt pathway in keratinocytes

The pathogenic effect of CEES on the keratinocytes is protein and lipid damage, loss of cell–cell communication and inflammation, which includes many complications in the skin and leading to skin injury. Therefore, we assessed that the involvement of inflammatory mediators in CEES-induced keratinocyte injury is mediated by Erk1/2-Akt pathway. CEES exposure at 1.5-mg doses resulted in a strong induction of TNFα, IL-1α, and ICAM (Fig. 7a). A similar kind of trend was observed in keratinocyte cells treated with increasing concentration of CEES for 24 h (data not shown). We also checked with Erk1/2 or Akt inhibitors whether the cytokines were augmented by CEES via Erk1/2-Akt pathway or not. As shown in Fig. 7b, pretreatment of cells with Erk1/2 or Akt inhibitors attenuated CEES-induced increase of TNFα, IL-1α, and ICAM expression in keratinocyte cells. Next, we measured the chemokines such as CXCL1, CCL8, and CXCL10 in the presence or absence of CEES. The expression of CXCL1 and CCL8 was downregulated, whereas CXCL10 expression was upregulated in the presence of 1.5-mg CEES exposure of mice skin tissues (Fig. 7c). However, pretreatment of cells with Erk1/2 or Akt inhibitor, U1 or Ly, attenuated the mRNA expression after 500 μM CEES exposure in keratinocyte cells (Fig. 7d). Further, we measured the MMPs after CEES exposure in keratinocytes. The CEES exposure at 1.5-mg doses resulted in a strong activation of MMP-2 and MMP-9 in skin tissues (Fig. 7e). However, treatment of cells with Erk1/2 or Akt inhibitors for 24 h attenuated the CEES-induced increase of MMP-2 and MMP-9 in HaCaT cells (Fig. 7f).

CEES exposure augments apoptosis via Erk1/2-Akt pathway in keratinocytes

Many lines of studies have reported in different cell types that CEES-induced cytotoxicity involves oxidative stress (Inturi et al. 2011; Naghii 2002). However, we hypothesized that CEES-induced oxidative stress and apoptosis are consequences of keratinocytes via

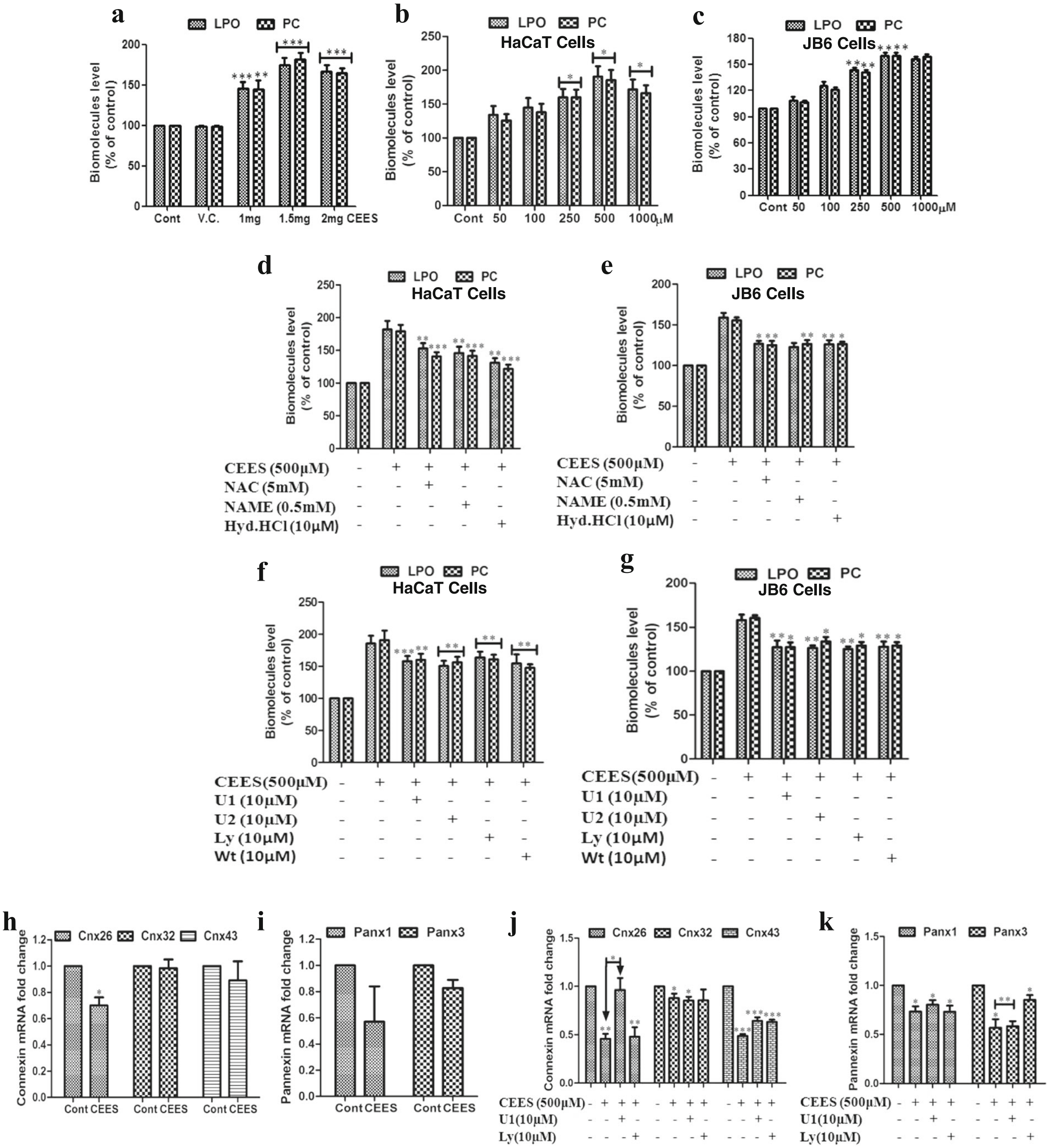

Fig. 6. CEES exposure augments oxidative stress which triggers biomolecular damage and is associated with loss of cell–cell communications via Erk11/2-Akt pathway in keratinocytes. Spectrophotometer assay showing increase in LPO and PC levels in SKH-1 hairless mice skin with exposure to increasing concentrations of CEES (**a**), and keratinocytes cells treated with increasing concentration of CEES (**b** and **c**). Pretreatment of NAC or NAME or Hyd·HCl inhibitors attenuated the CEES (500 μM) decrease in HaCaT (**d**) and JB6 cells (**e**). Pretreatment of Erk11/2 or Akt inhibitors attenuated the CEES (500 μM)-induced LPO and PC levels in HaCaT (**f**) and JB6 cells (**g**). QRT-PCR analysis of Cx26, Cx32, and Cx43 (**h**) and Panx1 and Panx3 (**i**) in mice skin tissues treated with 1.5 mg CEES. Pretreatment of Erk11/2 or Akt inhibitors attenuate the Cx26, Cx32, and Cx43 (**j**) and Panx1 and Panx3 mRNA expression (**k**) in HaCaT cells in the presence of 500 μM CEES. (***$p < 0.001$, **$p < 0.01$, and *$p < 0.05$)

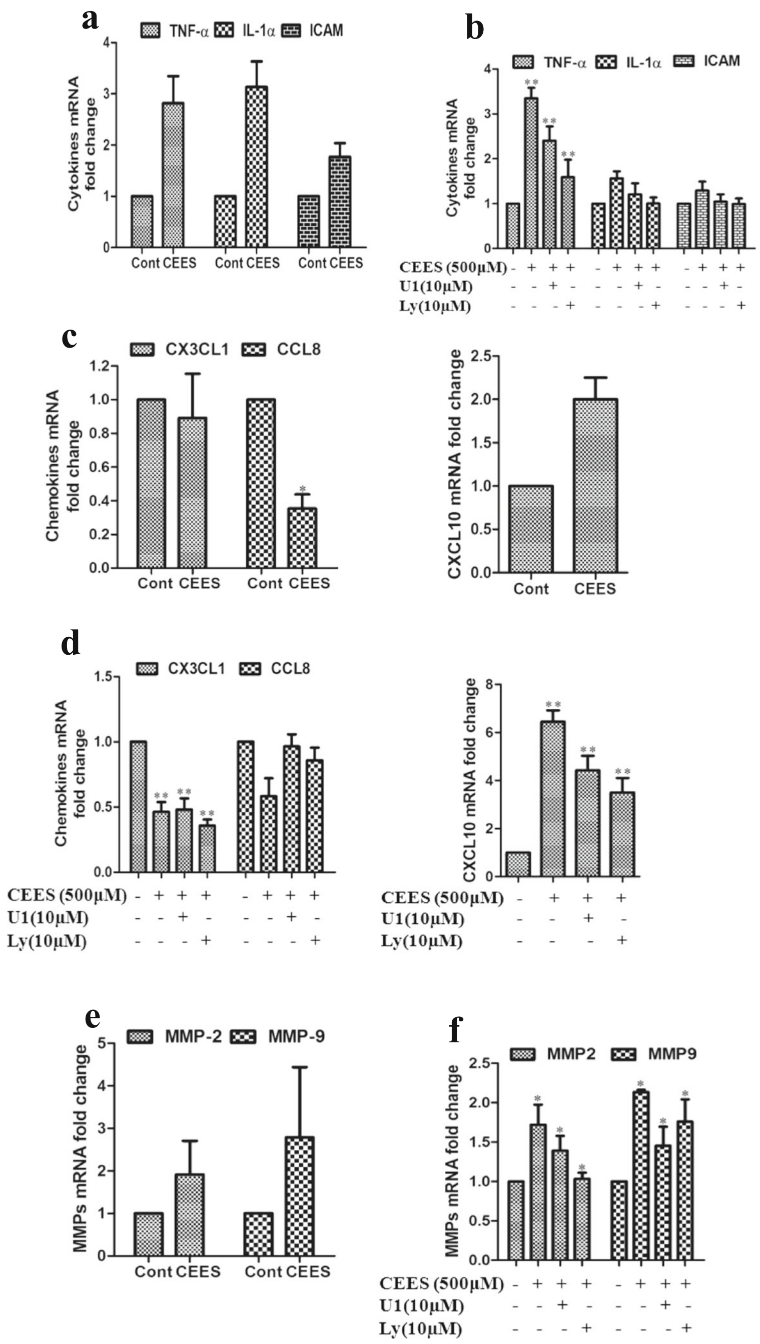

Fig. 7 CEES exposure augments oxidative stress which triggers expression of inflammatory mediators via Erk11/2-Akt pathway in keratinocytes. QRT-PCR analysis of TNFα, IL-1α, and ICAM in mice skin tissues treated with 1.5 mg CEES (**a**). Pretreatment of Erk11/2 or Akt inhibitors attenuate the TNFα, IL-1α, and ICAM mRNA expression in HaCaT cells in the presence of 500 μM CEES (**b**). (**$p < 0.01$ and *$p < 0.05$). QRT-PCR analysis of CXCL1, CCL8, and CXCL10 in mice skin tissues treated with 1.5 mg CEES (**c**). Pretreatment of Erk11/2 or Akt inhibitors attenuate the CXCL1, CCL8, and CXCL10 mRNA expression in HaCaT cells in the presence of 500 μM CEES (**d**). QRT-PCR analysis of MMP-2 and MMP-9 in mice skin tissues treated with 1.5 mg CEES (**e**). Pretreatment of Erk11/2 or Akt inhibitors attenuate the MMP-2 and MMP-9 mRNA expression in HaCaT cells in the presence of 500 μM CEES (**f**). (***$p < 0.001$, **$p < 0.01$, and *$p < 0.05$)

Erk1/2-Akt pathway. To examine CEES-caused apoptosis, first we assessed by MTT assay using JB6 and HaCaT cells. CEES exposure inhibited the proliferation of both keratinocyte cells (Fig. 8a). Further, to confirm that the CEES-induced apoptosis was regulated by oxidative stress, we incubated cells with NAC or NAME or Hyd·HCl in JB6 and HaCaT cells prior to CEES exposure. As shown in Fig. 8b and c, preincubation with ROS/RNS inhibitors with CEES attenuated the cell viability. Subsequently, we examined the CEES-induced oxidative stress via Erk1/2-Akt pathways. Both the cells were pretreated with various concentrations of Erk1/2 or Akt inhibitors. Almost all cytotoxic effects of 500 μM CEES were attenuated by U1 or U2 or Ly or Wt

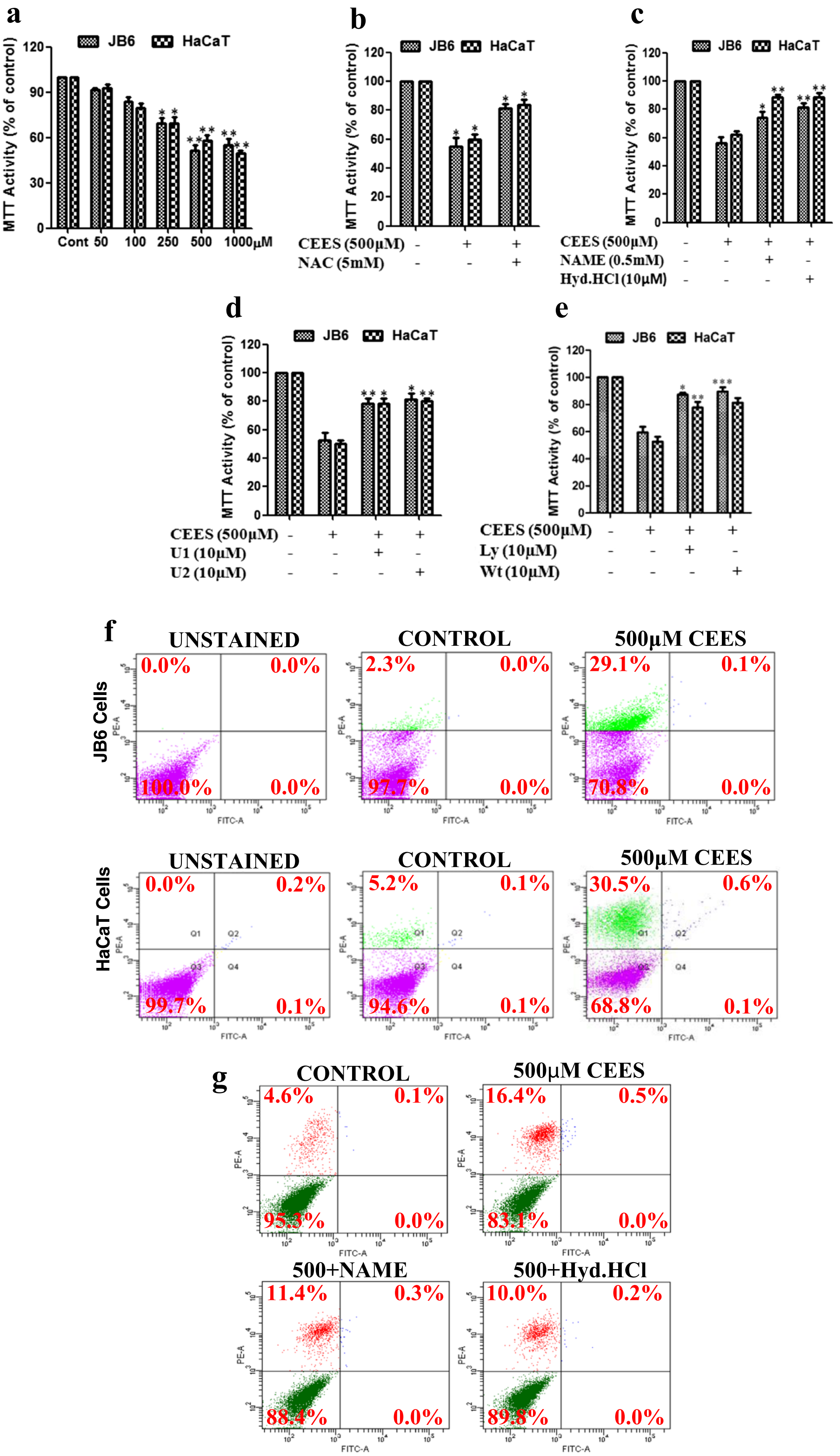
a
JB6 HaCaT
MTT Activity (% of control)
Cont 50 100 250 500 1000µM
b
CEES (500µM) - + +
NAC (5mM) - - +
c
CEES (500µM) - + + +
NAME (0.5mM) - - + -
Hyd.HCl (10µM) - - - +
d
CEES (500µM) - + + +
U1 (10µM) - - + -
U2 (10µM) - - - +
e
CEES (500µM) - + + +
Ly (10µM) - - + -
Wt (10µM) - - - +
f
JB6 Cells
UNSTAINED 0.0% 0.0% 100.0% 0.0%
CONTROL 2.3% 0.0% 97.7% 0.0%
500µM CEES 29.1% 0.1% 70.8% 0.0%
HaCaT Cells
UNSTAINED 0.0% 0.2% 99.7% 0.1%
CONTROL 5.2% 0.1% 94.6% 0.1%
500µM CEES 30.5% 0.6% 68.8% 0.1%
PE-A
FITC-A
g
CONTROL 4.6% 0.1% 95.3% 0.0%
500µM CEES 16.4% 0.5% 83.1% 0.0%
500+NAME 11.4% 0.3% 88.4% 0.0%
500+Hyd.HCl 10.0% 0.2% 89.8% 0.0%

◀ **Fig. 8** CEES exposure augments oxidative stress which triggers apoptosis via the Erk11/2-Akt pathway in keratinocytes. MTT assay showing the inhibition of cell proliferation of cells after CEES exposure in keratinocyte cells (**a**), and pretreatment of cells with NAC (**b**) and NAME or Hyd·HCl (**c**) in keratinocyte cells attenuated the cell viability after CEES exposure. Pretreatment of Erk11/2 (**d**) or Akt inhibitors (**e**) attenuates the cell death in keratinocyte cells in the presence of 500 μM CEES. A representative FACS analysis of apoptotic cell death after exposure of 500 μM CEES (**f**), and pretreatment of cells with NAME or Hyd·HCl (**g**) in HaCaT cells attenuated the apoptotic cell death after CEES exposure. A representative cell cycle analysis after exposure of 500 μM CEES with Erk11/2 or Akt inhibitors (**g**) in keratinocyte cells. A representative western blot of Chk1 and Chk2 with increasing concentration of CEES both in vivo and in vitro models (**i**). A representative lysosome content by autophagosome accumulation in CEES-treated keratinocyte cells with/without Erk11/2 or Akt inhibitors (**j**)

(Fig. 8d and e). Further, to better understand the increase in apoptotic cell death due to CEES with/without inhibitors, quantification of apoptotic cells was carried out. The cells were harvested after treatment with/without inhibitors, resuspended in binding buffer, and mixed with PI followed by diluting them with binding buffer, and fluorescent signals were detected apoptotic signal (Fig. 8f and g). To assess the growth inhibitory effect observed upon CEES treatments in keratinocytes, we performed cell cycle distribution assay with/without inhibitors in the presence or absence of CEES. As shown in Fig. S5, the cell cycle deregulation was observed with increasing concentration of CEES. To further confirm that the CEES effect on cell cycle deregulation was mediated by ROS and RNS production, keratinocyte cells were pretreated with Erk1/2 or Akt inhibitors before CEES exposure and then cell cycle analysis was investigated. We observed that 500 μM CEES exposed JB6 and HaCaT cells was showing increased percentage of S-phase, and reduced in G1 and G2/M-phase dose dependently, which restored using Erk1/2 or Akt inhibitors (Fig. 8h). Moreover, we evaluated few cell cycle modulators in mice and HaCaT cells including Chk1 and Chk2 by immunoblotting. Treatment with increasing concentration of CEES caused an increase in expression of these markers in both in vivo and in vitro models (Fig. 8i). Next, we observed another apoptotic marker, the changes in lysosome content by autophagosome accumulation and lysosome impairment in CEES-treated keratinocyte cells with/without inhibitors. Figure 8j illustrated that cells treated with 500 μM CEES boost more lysosomal staining compared with control, while in cells treated with NAC or NAME or Hyd·HCl or ERK1/2 or Akt inhibitors, the staining was reduced to that of control level restoring the lysosomal content of cells.

Discussion

Many lines of studies have reported the involvement of oxidative stress and the roles of MAPKs-Akt signaling pathways in CEES-induced inflammation, toxicity, and skin tissue injury (Pal et al. 2009; Tewari-Singh et al. 2009; Rebholz et al. 2008; Paromov et al. 2007). In fact, CEES is capable of inducing many inflammatory mediators and makes it very plausible that CEES activates not only the MAPKs-Akt pathways, largely involved in response to oxidative stress, but also causal to inflammation and apoptosis. In the present study, our results show that exposure of CEES to keratinocytes resulted in marked phosphorylation of Erk1/2 and Akt in both animal and cell culture models, indicating activation of Erk1/2-Akt signaling pathways. Our results are in agreement with the previous findings that Erk11/2-Akt pathway is triggered by CEES in different cell culture and animal models (Rebholz et al. 2008; Mukhopadhyay et al. 2008; Zhong et al. 2005).

Under normal physiological conditions, NO occurs in cellular compartments by the conversion of L-arginine to L-citrulline in the presence of NOS. In cellular compartments, iNOS is activated by a transient increase in cytosolic calcium in different cell types including keratinocytes, which promotes NO release (Kumar et al. 2017; Hur et al. 1998). Moreover, iNOS is expressed in different immunological cell types after exposure of CEES producing large amounts of NO (Sagar et al. 2014, 2017; Stone et al. 2003). In the present study, our results show that CEES exposure enhanced the iNOS expression in keratinocytes. Parallel with iNOS expression, the production of NO increased in keratinocytes after exposure of CEES. In contrast, NAME, a NO inhibitor, was widely used to inhibit NO production in different physiological conditions (Khan et al. 2016; Li et al. 2015). We also observed that pretreatment of NAME decreased the production of NO in keratinocyte cells after CEES exposure. On the other hand, NO is a free radical, associated with O2·– form ONOO–, a powerful oxidant in various inflammatory and pathological conditions that can attack a wide

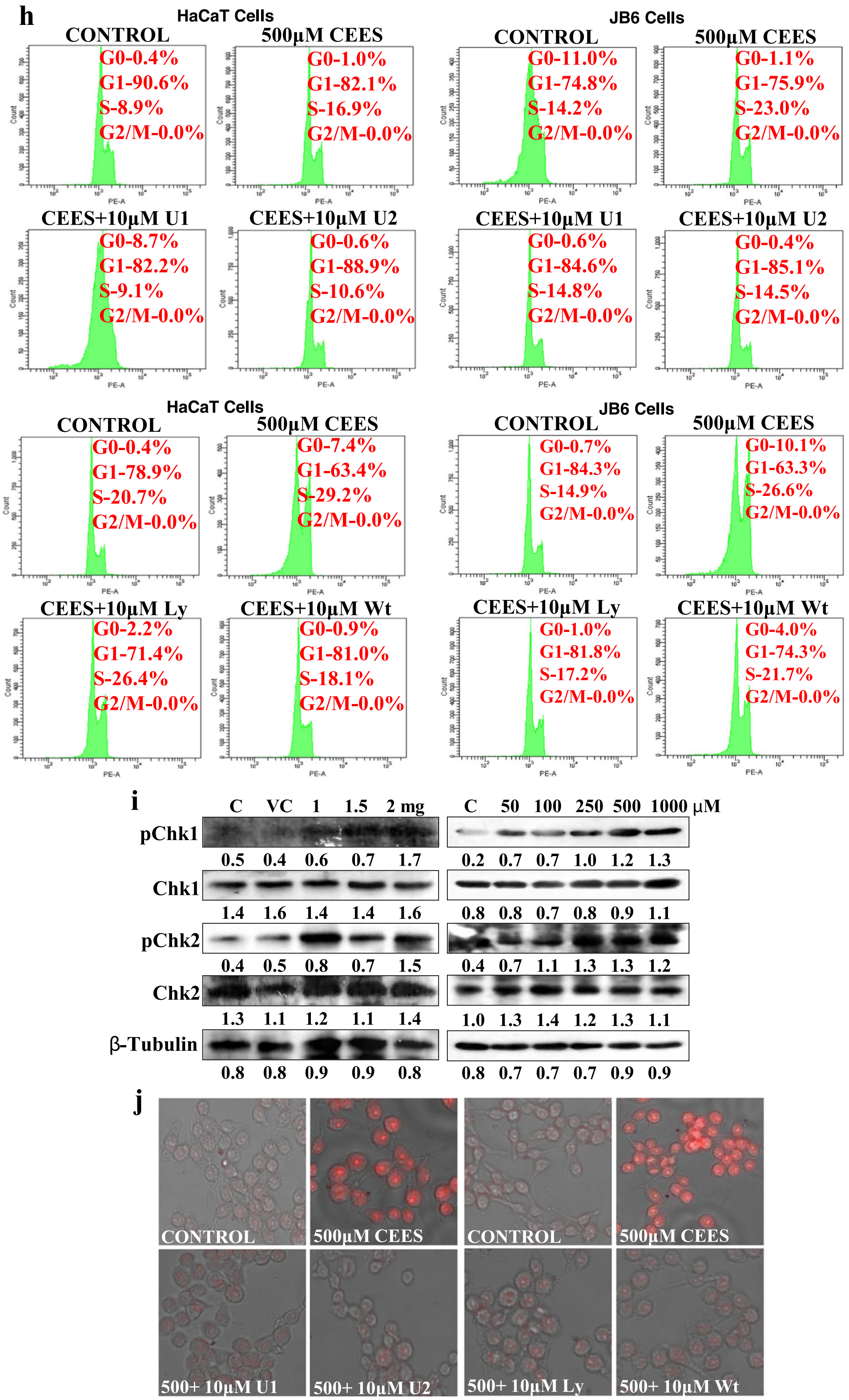

Fig. 8 continued.

variety of biological molecules (Carr et al. 2000). In this study, overproduction of O2·– and ONOO– was observed in keratinocyte cells after CEES exposure. However, pretreatment of NAC, O2·– inhibitor, or NO inhibitor NAME or ONOO– inhibitor Hyd·HCl attenuated the action. Finally, the cytotoxic signals of NO in keratinocytes after CEES administration, the reaction with O2·– was more relevant. The reaction product ONOO– supports the additional reactions through their interaction with targets via redox and additive chemistry in keratinocytes. Again, the CEES-induced free radical production in keratinocytes is mediated by Erk1/2-Akt pathways; we checked with Erk1/2 or Akt inhibitors whether the production and accumulation of free radicals were mediated by CEES via Erk1/2/Akt pathway or not. Pretreatment of cells with Erk1/2 or Akt inhibitors attenuated the CEES-induced production and accumulation of free radicals in keratinocyte cells.

Studies have shown that CEES exposure to different cell types triggered depletion of antioxidant capacities in cellular compartments (Gautam and Vijayaraghavan 2007). Specifically, GSH reduction may inhibit further clearance of CEES, and importantly, elicit oxidative stress, and biomolecule damage such as LPO, PC, and DNA (Pal et al. 2009; Laskin et al. 2010). Moreover, GSH acts as substrate for GPx, which detoxifies both H_2O_2 and lipid hydroperoxides to H_2O and alcohol (Arora et al. 2016; Bloodsworth et al. 2000). Similarly, CAT rapidly breaks up H_2O_2 to form H_2O and O_2 in cellular compartments. Here in our study, cellular antioxidant activities such as CAT, GSH, and GPx in keratinocyte cells subjected to CEES decreased with exposure of various concentrations of CEES. In line with these ideas, supplementation with NAC or NAME or Hyd·HCl protected against CEES-induced antioxidant depletion in keratinocytes. To further confirm that the CEES-induced antioxidant depletion in keratinocytes was mediated by Erk1/2-Akt pathways, we checked with Erk1/2 or Akt inhibitors whether the depletion of antioxidant capacity regulated by CEES induced oxidative stress via Erk11/2/Akt pathway or not. Pretreatment of cells with Erk1/2 or Akt inhibitors attenuated CEES-induced depletion of antioxidant capacity in keratinocyte cells.

In normal physiological conditions, the intracellular redox status of –SH is highly reductive. Earlier studies have suggested that the GSH was presented high concentrations in epithelial lining fluid and has been reported to maintain the integrity of epithelia (Cantin et al. 1989; Haddad and Harb 2005). On the other hand, Cys is an important amino acid in proteins that undergoes reversible oxidation/reduction reaction under different pathophysiological conditions and has been shown to not only control protein function, but also serve as a biomarker of oxidative damage (Liang and Patel 2016). More importantly, the ratio of Cys/Cys has been proposed to serve as a biomarker of redox status of different cells, tissues, and plasma in animals including humans (Go and Jones 2011). The presence of oxidative stress causes the S-glutathiolation of the critical Cys residue in the propeptide domain that disrupts its binding to the catalytic Zn2+ ion, resulting in an active full-length enzyme in cellular compartments. We have also checked the thiol amino acid metabolite depletion after treating with CEES in both in vitro and in vivo conditions in order to find the effect of CEES at metabolic level. GSH is the principal thiol antioxidant, and a key regulator of cellular protein thiol redox states (Schafer and Buettner 2001). Again, we observed that pretreatment of cells with NAC or NAME or Hyd·HCl or Erk1/2 or Akt inhibitors attenuated the CEES-induced depletion of GSH and Cys in keratinocytes. In addition to its direct antioxidant function, the synthesis of GSH from its rate-limiting substrate Cys minimizes the toxicity of excess Cys accumulation and acts as a cellular Cys reserve (Jones 2006). Cys exerts prooxidant effects in cells by oxidizing protein thiols through S-cysteinylation. Thus, a comprehensive analysis of amino acids, in addition to directly focusing on metabolites in the Arg and SAA pathways, may be useful in identifying factors that contribute to Arg and SAA pathway shifts on inflammation and apoptosis via oxidative stress and Erk1/2-Akt signaling pathway.

One of the regulators of glucose metabolism is the increase in Fru-2,6-P2 levels, which activates the flux through PFK-1. In many glycolytic cells, Fru-2,6-P2 levels are tightly regulated through balancing PFK-2/FBPase-2 activities. In mammals, four genes encode the PFK-2/FBPase-2. The L-type is encoded by the PFKB1 gene and is mainly expressed in the liver and muscle. The PFK-2 is encoded by the PFKB3 gene and has a predominantly kinase activity, with lower bisphosphatase activity. This gene is induced by stress stimuli and plays a key role in the high glycolytic rate. In cellular compartments, upon stimulation by CEES, switches the expression of the PFK-2/FBPase-2 isoform from PFKB1 to PFKB3, resulting in an increase in Fru-2,6-P2 levels and regulate glycolytic flux. Interestingly, MEK/Erk1/2 inhibition-dependent expression of uPFK-2 thus decreases Fru-2,6-P2 levels and PFK-2 activity in macrophages after infection (Través et al. 2012). Recently, studies have shown that under stress, PFKFB3 levels were high (Novellasdemunt et al. 2013). In the present study, we analyzed the mechanism of regulation of PFKFB3 as an immediate early gene controlled by CEES that activates through Erk1/2-Akt pathway. We report that exposure of keratinocytes to CEES leads to a rapid increase in PFKFB3 expression. The use of specific inhibitors such as NAC, NAME, U1, U2, Ly, and Wt in keratinocyte cells implicates control by the Erk1/2-Akt-regulated oxidative-nitrosative stress. Taken together, the results of the present study suggest a multimodal mechanism of stress stimuli induced by CEES affecting PFKFB3 transcriptional regulation, resulting in an increase in Fru-2,6-P2 concentration and stimulation of glycolysis in keratinocytes by Erk1/2-Akt pathway.

Several studies have shown that many inflammatory mediators could mediate oxidative stress signaling, and their participation of which in cellular pathways is modulated by cellular redox status (Haddad et al. 2001). In addition, cytokines are mediators of oxidative-nitrosative stress and can alter redox equilibrium by affecting GSH (Chen et al. 1998). Earlier reports suggested that ROS signaling pathways regulate the transcription of ILs and TNF-α, which was mediated by –SH-dependent mechanisms (Neuschwander-Tetri et al. 1996; Gosset et al. 1999). Elevated levels of cytokines and chemokines are hallmarks of chronic inflammation and are now responsible to promote the initiation and progression of skin injury after CEES exposure (Sabourin et al. 2002). On the other hand, in the event of cell death, various proinflammatory mediators including TNF-α and ILs were released into the extracellular matrix, activating the innate immune response. The role of oxygen radicals as secondary messengers for inducing expression of various inflammatory mediators in immunological cells was reported recently (Stone et al. 2003). In this study, our results indicate that CEES-induced oxidative stress triggers the activation of inflammatory cytokines such as TNF-α, IL-1α, ICAM, and chemokines including CX3CL-1, CXCL-10, and CCL-8 genes via key Erk1/2-Akt signaling pathways in keratinocytes. In addition, CEES treatment altered the cell-to-cell junction proteins, which were found to enhance the CEES-induced skin injury. Further, we observed that among several agents that were used for repletion and depletion of inflammation and cell-to-cell junction proteins, pretreatment of NAC, NAME, U1, U2, Ly, and Wt was particularly important as they exhibited antagonistic effects on a proinflammatory signal and cell-to-cell junction communication in the presence of CEES.

Apoptotic cell death due to CEES is accompanied by a series of complex biochemical events (Atkins et al. 2000). Our evaluation of cell viability and biochemical parameters revealed that CEES induces apoptotic cell death in keratinocytes. We also identified checkpoint kinase pathway leading to cell cycle arrest and apoptosis in keratinocytes. Further, we observed that the majority of the apoptotic cells were observed in the S-phase of the cell cycle in keratinocyte cells, whereas growth-arrested cells were predominantly in the G1 or G2/M-phase (Levrand et al. 2005; Beckman and Koppenol 1996). Further, we observed that pretreatment of NAC, NAME, U1, U2, Ly, and Wt is of particular importance as they exhibit antagonistic effects on an apoptosis in the presence of CEES. The lysosomal staining characteristic for apoptosis was clearly detected by CEES exposure, and pretreatment of inhibitors partially recovered the apoptotic cell death in keratinocyte cells. Hence, CEES-induced oxidative stress leads to disruption of Erk1/2-Akt signaling pathways, and increase in ROS/RNS production leads to antioxidant depletion, biomolecule damage, depletion in –SH metabolites, and decreased PFK-2 activity, gradually leading to inflammation, and loss of cell–cell communication leading to apoptosis. The identification of molecular mechanisms underlying keratinocytes gives insight into the pathogenesis of inflammatory mediator disorder leading to cell–cell communication and apoptosis via Erk1/2-Akt pathway in CEES-induced keratinocytes and may be useful to develop new therapeutic strategies against vesicant-induced skin injury.

Acknowledgements The authors gratefully acknowledge funding from the Indian Council of Medical Research (ICMR), grant 53/21/2010-CMB/BMS/ICMR, Government of India, to Dr. Arttatrana Pal.

Compliance with ethical standards

Specified protocol was approved by animal ethics approval at School of Biotechnology, KIIT.

Publisher's note Springer Nature remains neutral with regard to jurisdictional claims in published maps and institutional affiliations.

References

Albina JE, Mills CD, Henry WL Jr, Caldwell MD. Temporal expression of different pathways of 1-arginine metabolism in healing wounds. J Immunol. 1990;144:3877–80.

Arora D, Jain P, Singh N, Kaur H, Bhatla SC. Mechanisms of nitric oxide crosstalk with reactive oxygen species scavenging enzymes during abiotic stress tolerance in plants. Free Radic Res. 2016;50:291–303.

Atkins KB, Lodhi IJ, Hurley LL. Hinshaw DB. N-acetylcysteine and endothelial cell injury by sulfur mustard. J Appl Toxicol. 2000;20:S125–8.

Beckman JS, Koppenol WH. Nitric oxide, superoxide, and peroxynitrite: the good, the bad, and ugly. Am J Phys. 1996;271:C1424–37.

Bloodsworth A, O'Donnell VB, Freeman BA. Nitric oxide regulation of free radical- and enzyme-mediated lipid and lipoprotein oxidation. Arterioscler Thromb Vasc Biol. 2000;20: 1707–15.

Brosnan JT, Brosnan ME. The sulfur-containing amino acids: an overview. J Nutr. 2006;136:1636S–40S.

Calvo MN, Bartrons R, Castaño E, Perales JC, Navarro-Sabaté A, Manzano A. PFKFB3 gene silencing decreases glycolysis, induces cell-cycle delay and inhibits anchorage-independent growth in HeLa cells. FEBS Lett. 2006;580:3308–14.

Cantin AM, Hubbard RC, Crystal RG. Glutathione deficiency in the epithelial lining fluid of the lower respiratory tract in idiopathic pulmonary fibrosis. Am Rev Respir Dis. 1989;139:370–2.

Carr AC, McCall MR, Frei B. Oxidation of LDL by myeloperoxidase and reactive nitrogen species: reaction pathways and antioxidant protection. Arterioscler Thromb Vasc Biol. 2000;20:1716–23.

Chen CY, Huang YL, Lin TH. Association between oxidative stress and cytokine production in nickel-treated rats. Arch Biochem Biophys. 1998;356:127–32.

Cury-Boaventura MF, Curi R. Regulation of reactive oxygen species (ROS) production by C18 fatty acids in Jurkat and Raji cells. Clin Sci (Lond). 2005;108:245–53.

Ellman GL. Tissue sulfhydryl groups. Arch Biochem Biophys. 1959;82:70–7.

Finkelstein JD. Inborn errors of sulfur-containing amino acid metabolism. J Nutr. 2006;136:1750S–4S.

Gautam A, Vijayaraghavan R. Prophylactic effect of gossypin against percutaneously administered sulfur mustard. Biomed Environ Sci. 2007;20:250–9.

Go YM, Jones DP. Cysteine/cystine redox signaling in cardiovascular disease. Free Radic Biol Med. 2011;50:495–509.

Gosset P, Wallaert B, Tonnel AB, Fourneau C. Thiol regulation of the production of TNF-alpha, IL-6 and IL-8 by human alveolar macrophages. Eur Respir J. 1999;14:98–105.

Gould NS, White CW, Day BJ. A role for mitochondrial oxidative stress in sulfur mustard analog 2-chloroethyl ethyl sulfide-induced lung cell injury and antioxidant protection. J Pharmacol Exp Ther. 2009;328:732–9.

Haddad JJ, Harb HL. L-gamma-Glutamyl-L-cysteinyl-glycine (glutathione; GSH) and GSH-related enzymes in the regulation of pro- and anti-inflammatory cytokines: a signaling transcriptional scenario for redox(y) immunologic sensor(s)? Mol Immunol. 2005;42:987–1014.

Haddad JJ, Safieh-Garabedian B, Saadé NE, Land SC. Thiol regulation of pro-inflammatory cytokines reveals a novel immunopharmacological potential of glutathione in the alveolar epithelium. J Pharmacol Exp Ther. 2001;296:996–1005.

Hasarmeh M, Itzik A, Weidenfeld J, Ovadia H. Modulation of hyperosmotic and immune-induced disruption of the blood-brain barrier by the nitric oxide system. Neuroimmunomodulation. 2016;23:1–7.

Hur GH, Kim YB, Choi DS, Kim JH, Shin S. Apoptosis as a mechanism of 2-chloroethylethyl sulfide-induced cytotoxicity. Chem Biol Interact. 1998;110:57–70.

Inturi S, Tewari-Singh N, Gu M, Shrotriya S, Gomez J, Agarwal C, et al. Mechanisms of sulfur mustard analog 2-chloroethyl ethyl sulfide-induced DNA damage in skin epidermal cells and fibroblasts. Free Radic Biol Med. 2011;51:2272–80.

Jones DP. Redefining oxidative stress. Antioxid Redox Signal. 2006;8:1865–79.

Khan MI, Ostadhadi S, Zolfaghari S, Ejtemaei MS, Hassanzadeh G, Dehpour AR. The involvement of NMDA receptor/NO/cGMP pathway in the antidepressant like effects of baclofen in mouse force swimming test. Neurosci Lett. 2016;612:52–61.

Kim HG, Shrestha B, Lim SY, Yoon DH, Chang WC, Shin DJ, et al. Cordycepin inhibits lipopolysaccharide-induced inflammation by the suppression of NF-kappaB through Akt and p38 inhibition in RAW 264.7 macrophage cells. Eur J Pharmacol. 2006;545:192–9.

Kumar P, Swain MM, Pal A. Hyperglycemia-induced inflammation caused down-regulation of 8-oxoG-DNA glycosylase levels in murine macrophages is mediated by oxidative-nitrosative stress-dependent pathways. Int J Biochem Cell Biol. 2016;73:82–98.

Kumar P, Raman T, Swain MM, Mishra R, Pal A. Hyperglycemia-induced oxidative-nitrosative stress induces inflammation and neurodegeneration via augmented tuberous sclerosis complex-2 (TSC-2) activation in neuronal cells. Mol Neurobiol. 2017;54:238–54.

Laskin DL, Sunil VR, Fakhrzadeh L, Groves A, Gow AJ, Laskin JD. Macrophages, reactive nitrogen species, and lung injury. Ann N Y Acad Sci. 2010;1203:60–5.

Levrand S, Pesse B, Feihl F, Waeber B, Pacher P, Rolli J, et al. Peroxynitrite is a potent inhibitor of NF-{kappa}B activation triggered by inflammatory stimuli in cardiac and endothelial cell lines. J Biol Chem. 2005;280:34878–87.

Li S, Xu J, Yao W, Li H, Liu Q, Xiao F, et al. Sevoflurane pretreatment attenuates TNF-α-induced human endothelial cell dysfunction through activating eNOS/NO pathway. Biochem Biophys Res Commun. 2015;460:879–86.

Liang LP, Patel M. Plasma cysteine/cystine redox couple disruption in animal models of temporal lobe epilepsy. Redox Biol. 2016;9:45–9.

Manikandan R, Thiagarajan R, Beulaja S, Sudhandiran G, Arumugam M. Curcumin prevents free radical-mediated cataractogenesis through modulations in lens calcium. Free Radic Biol Med. 2010;48:483–92.

Meister A. Selective modification of glutathione metabolism. Science. 1983;220:472–7.

Morris SM Jr, Kepka-Lenhart D, Chen LC. Differential regulation of arginases and inducible nitric oxide synthase in murine macrophage cells. Am J Phys. 1998;275:E740–7.

Mukhopadhyay S, Mukherjee S, Smith M, Das SK. Activation of MAPK/AP-1 signaling pathway in lung injury induced by 2-chloroethyl ethyl sulfide, a mustard gas analog. Toxicol Lett. 2008;181:112–7.

Mytych J, Wnuk M, Rattan SI. Low doses of nanodiamonds and silica nanoparticles have beneficial hormetic effects in normal human skin fibroblasts in culture. Chemosphere. 2016;148:307–15.

Naghii MR. Sulfur mustard intoxication, oxidative stress, and antioxidants. Mil Med. 2002;167:573–5.

Neuschwander-Tetri BA, Bellezzo JM, Britton RS, Bacon BR, Fox ES. Thiol regulation of endotoxin-induced release of tumour necrosis factor alpha from isolated rat Kupffer cells. Biochem J. 1996;320:1005–10.

Novellasdemunt L, Bultot L, Manzano A, Ventura F, Rosa JL, Vertommen D, et al. PFKFB3 activation in cancer cells by the p38/MK2 pathway in response to stress stimuli. Biochem J. 2013;452:531–43.

Pal A, Tewari-Singh N, Gu M, Agarwal C, Huang J, Day BJ, et al. Sulfur mustard analog induces oxidative stress and activates signaling cascades in the skin of SKH-1 hairless mice. Free Radic Biol Med. 2009;47:1640–51.

Paromov V, Suntres Z, Smith M, Stone WL. Sulfur mustard toxicity following dermal exposure: role of oxidative stress, and antioxidant therapy. J Burns Wounds. 2007;7:e7.

Pastore A, Massoud R, Motti C, Lo RA, Fucci G, Cortese C, et al. Fully automated assay for total homocysteine, cysteine, cysteinylglycine, glutathione, cysteamine, and 2-mercaptopropionylglycine in plasma and urine. Clin Chem. 1998;44:825–32.

Rebholz B, Kehe K, Ruzicka T, Rupec RA. Role of NF-kappaB/RelA and MAPK pathways in keratinocytes in response to sulfur mustard. J Invest Dermatol. 2008;128:1626–32.

Rider MH, Bertrand L, Vertommen D, Michels PA, Rousseau GG. Hue L. 6-phosphofructo-2-kinase/fructose-2,6-bisphosphatase: head-to-head with a bifunctional enzyme that controls glycolysis. Biochem J. 2004;381:561–79.

Rodríguez-Prados JC, Través PG, Cuenca J, Rico D, Aragonés J, Martín-Sanz P, et al. Substrate fate in activated macrophages: a comparison between innate, classic, and alternative activation. J Immunol. 2010;185:605–14.

Sabourin CL, Danne MM, Buxton KL, Casillas RP, Schlager JJ. Cytokine, chemokine, and matrix metalloproteinase response after sulfur mustard injury to weanling pig skin. J Biochem Mol Toxicol. 2002;16:263–72.

Sagar S, Kumar P, Behera RR, Pal A. Effects of CEES and LPS synergistically stimulate oxidative stress inactivates OGG1 signaling in macrophage cells. J Hazard Mater. 2014;278:236–49.

Sagar S, Parida SR, Sabnam S, Rizwan H, Pal S, Swain MM, et al. Increasing NO level regulates apoptosis and inflammation in macrophages after 2-chloroethyl ethyl sulphide challenge. Int J Biochem Cell Biol. 2017;83:1–14.

Schafer FQ, Buettner GR. Redox environment of the cell as viewed through the redox state of the glutathione disulfide/glutathione couple. Free Radic Biol Med. 2001;30:1191–212.

Shaulian E, Karin M. AP-1 in cell proliferation and survival. Oncogene. 2001;20:2390–400.

Stone WL, Qui M, Smith M. Lipopolysaccharide enhances the cytotoxicity of 2-chloroethyl ethyl sulfide. BMC Cell Biol. 2003;4:1.

Tawakol A, Singh P, Mojena M, Pimentel-Santillana M, Emami H, MacNabb M, et al. HIF-1α and PFKFB3 mediate a tight relationship between proinflammatory activation and anerobic metabolism in atherosclerotic macrophages. Arterioscler Thromb Vasc Biol. 2015;35:1463–71.

Tewari-Singh N, Rana S, Gu M, Pal A, Orlicky DJ, White CW, et al. Inflammatory biomarkers of sulfur mustard analog 2-chloroethyl ethyl sulfide-induced skin injury in SKH-1 hairless mice. Toxicol Sci. 2009;108:194–206.

Tewari-Singh N, Gu M, Agarwal C, White CW, Agarwal R. Biological and molecular mechanisms of sulfur mustard analogue-induced toxicity in JB6 and HaCaT cells: possible role of ataxia telangiectasia-mutated/ataxia telangiectasia-Rad3-related cell cycle checkpoint pathway. Chem Res Toxicol. 2010;23:1034–44.

Tewari-Singh N, Jain AK, Inturi S, Agarwal C, White CW, Agarwal R. Silibinin attenuates sulfur mustard analog-induced skin injury by targeting multiple pathways connecting oxidative stress and inflammation. PLoS One. 2012;7:e46149.

Través PG, de Atauri P, Marín S, Pimentel-Santillana M, Rodríguez-Prados JC, de Marín MI, et al. Relevance of the MEK/ERK signaling pathway in the metabolism of activated macrophages: a metabolomic approach. J Immunol. 2012;188:1402–10.

Van Schaftingen SE, Jett MF, Hue L, Hers HG. Control of liver 6-phosphofructokinase by fructose 2,6-bisphosphate and other effectors. Proc Natl Acad Sci. 1981;78:3483–6.

Wang C, Youle RJ. The role of mitochondria in apoptosis. Annu Rev Genet. 2009;43:95–118.

Wright SK, Viola RE. Evaluation of methods for the quantitation of cysteines in proteins. Anal Biochem. 1998;265:8–14.

Yalcin A, Clem BF, Imbert-Fernandez Y, Ozcan SC, Peker S, O'Neal J, et al. 6-Phosphofructo-2-kinase (PFKFB3) promotes cell cycle progression and suppresses apoptosis via Cdk1 mediated phosphorylation of p27. Cell Death Dis. 2014;5:e1337.

Yoo BK, Choi JW, Han BH, Kim WK, Kim HC, Ko KH. Role of MAPK/ERK1/2 in the glucose deprivation-induced death in immunostimulated astroglia. Neurosci Lett. 2005;376:171–6.

Zhong CY, Zhou YM, Douglas GC, Witschi H, Pinkerton KE. MAPK/AP-1 signal pathway in tobacco smoke-induced cell proliferation and squamous metaplasia in the lungs of rats. Carcinogenesis. 2005;26:2187–95.